AJPS

e-ISSN: 2980-0463
Volume 2 / Issue 1

Anatolian Journal of Pharmaceutical Sciences

Inonu University
Faculty of Pharmacy
Turkey

Editorial Board

Chief Editor

Prof. Dr. Kadir BATÇIOĞLU

Editor-in-Chief

Assoc. Prof. Dr. Ebru KUYUMCU SAVAN

Section Editors

Assoc. Prof. Dr. Selami GÜNAL

Assoc. Prof. Dr. Emine ŞALVA

Assoc. Prof. Dr. Zeynep ÖZDEMİR

Copyeditors

Assoc. Prof. Dr. A. Burçin UYUMLU

Asst. Prof. Dr. Emre UYAR

Asst. Prof. Dr. Zehra TORUN

Language Editors

Asst. Prof. Dr. Hayrettin TONBUL

Asst. Prof. Dr. Gözde ULTAV

Layout Editor

Yaren Nur ZENNİ

Secretary

Muhammet Burak AÇIKGÜL

Dilek KAZICI

Contents

1. **Research Article: Narin SADIKOGLU,** Investigation of the Awareness Level of the Medicinal and Aromatic Plants Garden of Inonu University Faculty of Pharmacy on the Students of the Faculty of Pharmacy.
2. **Research Article: Esma KARACA KARADOGAN, Zeynep OZDEMIR, Yaren Nur ZENNI, Arzu KARAKURT,** Enantioseparation of 2-(1*H*-imidazol-1-yl)-1-(naphthalen-2-yl)ethan-1-ol which is active metabolite of anticonvulsant nafimidone.
3. **Research Article: Sema ZABCI, Azra RAFIQ, Semra KOCABIYIK,** Structural and Functional Impacts of the Altered Hydrophobicity in the Dimer Interface of *Tpv* HSP 14.3.
4. **Research Article: Kadir BATCIOGLU, Mehmet TECELLIOGLU,** Design and Development of a Prototype of Programmable Tracheostomy Cannula that can Perform Over-Cuff Suction for Use in Intensive Care Patients with Dysphagia.
5. **Review Article: Özlem Çankaya,** Biochemistry of the Human Lens.

e-ISSN: 2980-0463
Anat. J. Pharm. Sci 2023:2(1)
AJPS
Research Article

Investigation of the Awareness Level of the Medicinal and Aromatic Plants Garden of Inonu University Faculty of Pharmacy on the Students of the Faculty of Pharmacy

Narin SADIKOGLU*

* Department of Pharmacognosy, Faculty of Pharmacy, Inonu University, Malatya, Türkiye

ABSTRACT: A survey study was conducted to shed light on the accreditation studies of the Faculty of Pharmacy of Inonu University and to determine the awareness level of the Medicinal and Aromatic Plants Garden of the faculty's on the faculty students. According to the data of the study in which 242 students participated, the courses taken in the Medicinal and Aromatic Plants Garden of Faculty of Pharmacy made a full contribution to the students getting to know the medicinal plants better and easily remembering the active ingredient contents when they saw the plant. The existence of the garden encourages most students to take further education in medicinal plants, and to grow medicinal plants as well as to prepare and sell herbal products when they own a pharmacy.

Key Words: Students of faculty of pharmacy, Inonu University Faculty of Pharmacy, medicinal plants, medicinal and aromatic plants garden, Malatya.

1 INTRODUCTION

Especially in recent years, it is seen that the public is exposed to information that is far from the truth about medicinal plants due to popular sources written by non-experts, television programs and even social media contents. However, in the Faculties of Pharmacy, which is the only place where education is given on indications, contraindications, side effects, interactions with drugs, food and other plants of medicinal plants, students graduate with the theoretical and practical training they receive in the classrooms and in the laboratories [1]. On the other hand, in faculties that have a garden where medicinal and aromatic plants are grown, students receive practical training in the garden in addition to these and graduate with their knowledge reinforced. In addition, students from primary school to high school visiting the garden, the teachers who accompany them and those who are interested in amateurs will have the opportunity to correct their environmental misconceptions and incomplete knowledge, as well as some useful information they will add to their daily lives [2].

*Corresponding Author: Narin SADIKOGLU
E-mail: narin.sadikoglu@inonu.edu.tr
Submitted: 29.08.2023 Accepted: 11.10.2023

Herbal drugs are very important in pharmacy education. Medicinal and Aromatic Plants Garden of Inonu University Faculty of Pharmacy, is a laboratory where the plants are shown in live form to the students who take the courses of Pharmacognosy and Pharmaceutical Botany Departments and contribute to education. An important part of the herbal materials required for student laboratories are provided here [3]. All or parts of the lessons on medicinal plants are held in the garden. Especially, students who prepare a graduation thesis in their last year have the chance to experience the stages from seed to product. In addition, students who wish can work voluntarily in the garden.

Inonu University Faculty of Pharmacy was accredited in 2023 [4]. In this process, various opinions were taken from the students in order to contribute to the development and sustainability studies. In this study, it was aimed to investigate the contribution of the Medicinal and Aromatic Plants Garden in the Faculty of Pharmacy of Inonu University to the awareness levels of the students of the Faculty of Pharmacy.

This study was presented as an oral presentation at the 3rd National Botanical Gardens Symposium (Gaziantep- 23-25 March 2022), but it has not been published anywhere before because no summary or full-text book of proceedings was prepared for the meeting [5].

2 MATERIALS AND METHODS

A questionnaire containing 31 questions was applied to the 3rd, 4th and 5th grade students of the faculty, stating that it would be used in the accreditation process and shared in the scientific environment, with the permission of the dean's office. The reason for choosing these classes is that during the study period, there is a compulsory course to be held in the garden in the 4th grade, in addition to the elective courses in the garden in the 5th grade, these students took courses in the garden the previous year and there were no courses to be held in the garden in the 3rd grade. Thus, in order to make an objective comparison of the effect of taking courses in the garden, three classes consisting of those who have taken one or more courses and those who have never seen them have been selected. The reason why 1st and 2nd year students were excluded from the study is that they are not very familiar with the faculty. Because the 2nd year students were restricted due to the pandemic in the year they enrolled in the faculty and were still in the adaptation process like the 1st year students.

When the spring semester of the 2021-2022 academic year started, each class was given a question paper before the lesson and they were immediately answered, and it was collected back and applied to the students who did not come in the next lesson. There was no one who did not want to participate in the survey, and everyone answered helpfully. It was aimed for all students to participate in the study, but 31 students could not participate because they did not come to faculty due to reported illness, registration freeze and absenteeism. Of the survey questions, 10 of them have 2 point (Yes / No) answers and 20 of them have 5 point (Strongly agree / Agree / Undecided / Disagree / Strongly Disagree) answer options. Only gender information was asked as a demographic question. Name, number or any contact information was not taken in order to reflect the truth without hesitation while answering. The questions were not taken from anywhere; they were prepared by the author completely amateurishly and in accordance with the purpose.

3 RESULTS AND DISCUSSION

As of February 2022, there are a total of 485 students, 308 females and 177 males, at the faculty (Figure 1.A). Among the students, 273 of these students are 3rd, 4th, and 5th grade students and it is aimed to apply a questionnaire (Table 1). A total of 242 students, 93 from the 3rd grade, 90 from the 4th grade, and 59 from the 5th grade, participated in the survey. A total of 31 students, 9 from the 3rd grade and 22 from the 5th grade, could not be surveyed (Table 2). Although there is no course to be held in the garden of the 3rd grade, 4 students from the 3rd grade have taken courses in the garden and the reason is that they have taken the 4th grade upper class. Although there was a course to be held in the garden of the 4th grade, 6 students from the 4th grade did not take a course in the garden. These are the students who could not take courses because their credits were not enough, but they voluntarily helped with gardening. Of the students, 124 students took courses, 118 did not (Figure 1.B). The number of students who stated that they worked voluntarily outside the scope of the course was 74 (Figure 2.A). Considering the distribution according to classes, it was determined that 7 students from the 3rd grade, 41 from the 4th grade and 26 students from the 5th grade worked voluntarily. When asked whether they would like to help with gardening voluntarily, the majority of the 5th graders (36 students) stated that they wanted to volunteer, while the rate of willingness was half in the 3rd and 4th grades (Figure 2.B).

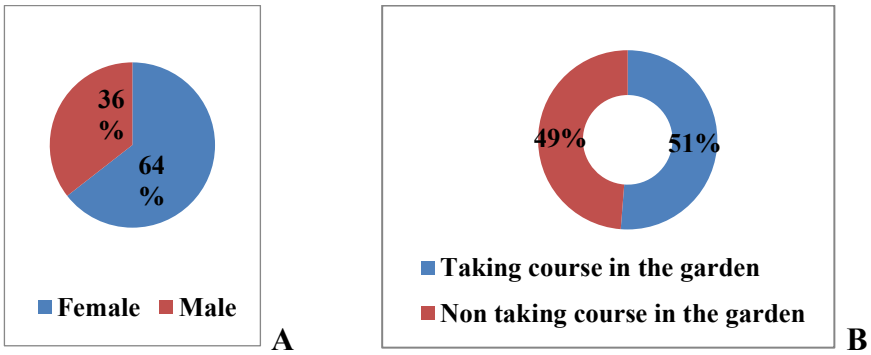

Figure 1. Distribution of students participating in the survey **A.** Gender, **B.** Course taking.

Table 1. Distribution of faculty students.

Faculty Students	Current	Aimed to be survey	Surveyed
Female	308	174	156
Male	177	99	86
Total	**485**	**273**	**242**

Table 2. Distribution of the students who were surveyed.

Classes	Gender	Current	Surveyed		
			Total	Taking Course	Non Taking Course
3	Female	63	58	3	55
	Male	39	35	one	34
	Total	**102**	**93**	**4**	**89**
4	Female	59	59	58	one
	Male	31	31	26	5
	Total	**90**	**90**	**84**	**6**
5	Female	52	39	24	15
	Male	29	20	12	8
	Total	**81**	**59**	**36**	**23**
Total		**273**	**242**	**124**	**118**

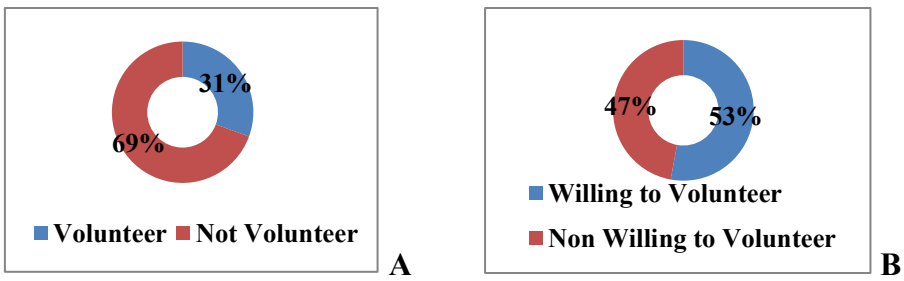

Figure 2. A. Volunteering, **B.** Willingness to volunteer.

When asked if they wanted courses in the garden, 80% gave a positive answer, and 82% when asked if they wanted to increase the number of courses to be taught in the garden (Figure 3.A, B). The number of students with soil experience is more than half in each class (Figure 4.A). It was clearly seen that the students who worked in the field or in the garden easily did the work in the faculty garden compared to the others. The number of those who intend to produce medicinal plants in the future is 191, 72 students from each of the 3rd and 4th grades, and 47 students from the 5th grade (Figure 4.B).

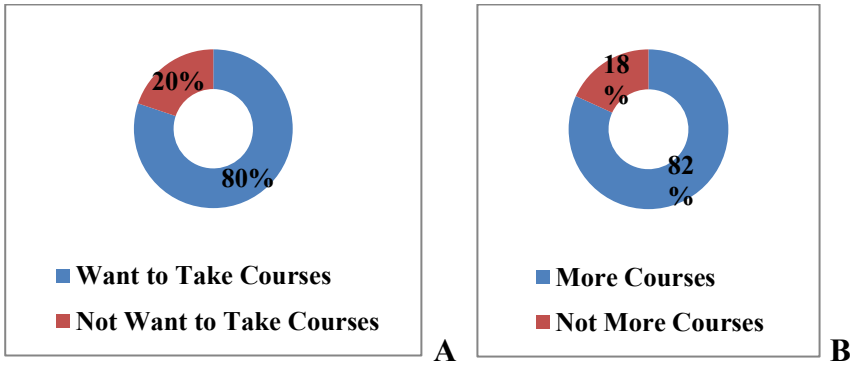

Figure 3. A. Desire to take courses in the garden, **B.** Desire to take more courses in the garden.

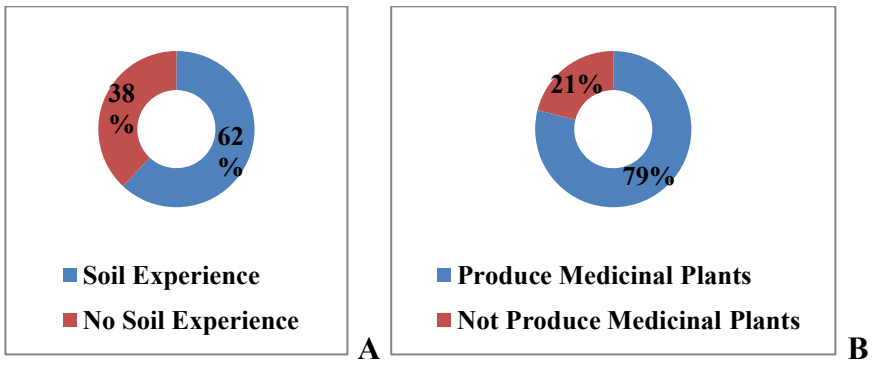

Figure 4. A. Soil experience, **B.** Production will.

The number of those who think to include herbal products when they own a pharmacy is 231, and 2 students from the 3rd grade, 6 from the 4th grade and 3 from the 5th grade stated that they do not want to sell (Figure 5.A). Those who think about preparing

herbal products in their pharmacies are again in the majority and those who stated that they do not want are 6 students from the 3rd grade, 12 from the 4th grade and 3 from the 5th grade (Figure 5.B). The rate of those who are considering taking postgraduate education (in-service training, courses, graduate degrees, etc.) on medicinal plants is 76% (Figure 5.C). Of those who stated that they do not intend to receive education, 27 are from the 3rd grade, 20 from the 4th grade, and 10 from the 5th grade. When students move on to advanced classes, an increase in their desire for education is observed. Since a quarter of the seniors did not participate in the survey, it can be expected that this rate would increase even more if they did.

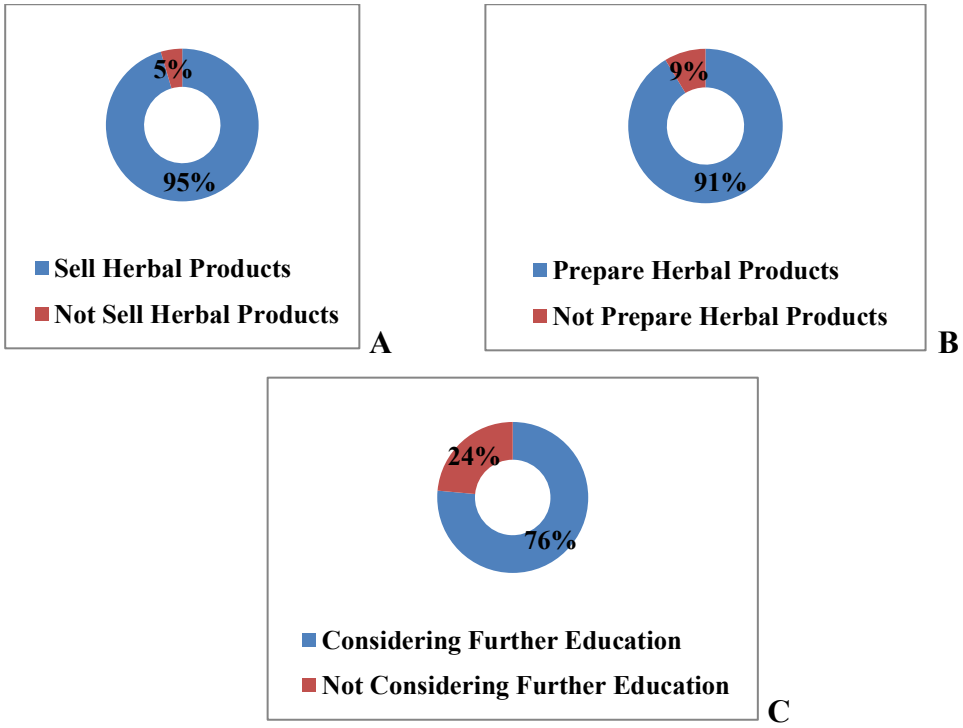

Figure 5. A. Willingness to sell, **B.** Willingness to prepare, **C.** Training prompt.

Almost all students (except 1-3 students from each class) think that with taking courses in the garden, they will be able to recognize medicinal plants better, remember the names of medicinal plants more easily, keep their effects in mind more easily, to have an idea about growing medicinal plants and increase their knowledge in the process starting from seed to product development. They also mostly agree that dealing with the soil will reduce stress, enjoy drinking the tea of the plants they have helped to grow, also enjoy developing products from these plants and, that taking courses in the garden will positively affect their success in the exam. Those who did not participate are mostly from the 3rd grade students who did not take lessons in the garden.

It has been determined that they do not have much knowledge about soil conditions required for growing medicinal plants, and drug collection and preparation. It is a known fact that especially graduates of Medicinal and Aromatic Plants Cultivation department will have full knowledge on this subject. Although the students of the Faculty of Pharmacy are not expected to have a good command of the subject, these questions were included in the questionnaire in order to observe the change in the situation as they take more courses in the garden in the future. It has been observed that this knowledge, which the uneducated can acquire by practicing and spending a lot of time in the garden, is 1/3 even among the students who have taken courses in the garden, but it has been clearly observed that as the experience increases, those who work as extra volunteers outside of class hours have clearly shown improvement. Students working in the garden have become able to recognize some important medicinal plants when they see them in nature. They state that they can recognize some important plants used in the preparation of medicinal teas and as spices, as well as some poisonous plants. Among those who do not work in the garden, the number of those who say they can recognize them is less. These students are 3rd year students who have seen plants in theoretical courses and have come to the garden only for visiting purposes. It is seen from the answers they give that they want to be in the garden even though they had not yet taken a course in the garden, and that they envy those who take courses.

There were also students (12 from 3rd grade, 21 from 4th grade, 7 from 5th grade) who stated that they did not agree, although they were expected to participate in professional matters such as herbal

products are important in treatment, herbal medicines have therapeutic effects, and counseling the patient about the use and effect of medicinal plants is among the duties of the pharmacist. Those who are undecided on these issues are 20 students from the 3rd grade, 30 students from the 4th grade, and 15 students from the 5th grade. Most of the students think that herbal medicine or natural products will take place more in pharmacies in the future. Those who do not think are 11 students; those who are undecided are 20.

It was planned to develop the questionnaire and repeat it every year at the end of the year, to increase the quality of education in the garden accordingly, and to publish the results on the faculty website. In addition, it is thought that conducting a survey for each course to be held in the garden and publishing the results by combining them will encourage the opening of new courses and the improvement of the existing ones.

4 CONCLUSIONS

It has been determined that the students are generally satisfied with working in the garden, they want to take more courses in the garden, they take the stress of dealing with gardening, they like to develop products from the plants they contribute to their growth, they want to prepare and sell herbal products in their pharmacies and grow medicinal plants in the future. It has been concluded that the presence of the Medicinal and Aromatic Plants Garden in the faculty contributes to better knowing the plants and the success rate in the exams. It is clearly seen from the answers given by the students who have taken courses in the garden and those who have not, that teaching in the garden contributes to the student. It is possible to say that the existence of the garden creates an awareness compared to the absence of a garden, even for the students who have not taken a course in the garden.

Medicinal plant gardens are very important for Pharmacy Faculties. Cultivating the plants used in drug making, like the old pharmacists, will provide an advantage to the students in terms of both predisposing to the preparation of magistral drugs and being ready for the processes in the preparation of traditional herbal medicinal products. The establishment of these gardens in other Pharmacy Faculties should be encouraged.

5 ACKNOWLEDGMENTS

I would like to thank to Prof. Dr. Kadir BATÇIOĞLU, dean of the faculty who gave me the idea to create this work

and the faculty accreditation committee members for their support in preparing the survey questions.

6 AUTHOR CONTRIBUTIONS

Hypothesis: N.S.; Design: N.S.; Literature review: N.S.; Data Collection: N.S.; Analysis and/or interpretation: N.S.; Manuscript writing: N.S.

7 CONFLICT OF INTEREST

The author declares that there is no conflict of interest.

8 REFERENCES

[1] Anonim. ECZAKDER Öz Değerlendirme Raporu, İnönü Üniversitesi Eczacılık Fakültesi, 2022.

[2] Sadıkoğlu N. İnönü Üniversitesi Tıbbi ve Aromatik Bitkiler Bahçesi Oluşturulması. Malatya, İnönü Üniversitesi BAP, Güdümlü Proje No: 2013/34, 2016.

[3] Sadıkoğlu, N. Yeniden Canlandırma Sürecinde İnönü Üniversitesi Tıbbi ve Aromatik Bitkiler Bahçesi. Ulusal Botanik Bahçeleri, Arboretumlar, Herbaryumlar ve Botanik Müzeleri Çalıştayı, 18-21 April 2019, Düzce, Proceeding Book, 78.

[4] https://www.inonu.edu.tr/eczacilik/ 23 June 2023

[5] https://ubbs2022.com/Sempozyum/sempozyum-programi/15/18 March 2022

e-ISSN: 2980-0463
Anat. J. Pharm. Sci 2023:2(1)
AJPS
Research Article

Enantioseparation of 2-(1*H*-imidazol-1-yl)-1-(naphthalen-2-yl)ethan-1-ol which is active metabolite of anticonvulsant nafimidone

Esma KARACA KARADOGAN[1], Zeynep OZDEMIR[1*], Yaren Nur ZENNI[1], Arzu KARAKURT[1]

[1*] Department of Pharmaceutical Chemistry, Faculty of Pharmacy, Inonu University, Malatya, Türkiye

ABSTRACT: Nafimidone and nafimidone alcohol, which were synthesized in 1981 and whose anticonvulsant activities were determined, are important anticonvulsant compounds in the structure of (arylalkyl)azole, which reached the stage of clinical human studies but could not pass this stage. In this study, the commercially available chiral stationary phase amylose tris(3,5-dimethyphenylcarbamate) (Chiralpak AD) was used to establish direct enantiomeric separations of nafimidone alcohol which is the metabolite of nafimidone in the normal phase HPLC mode. Investigations were also done into the compositional influences of the mobile phase. When the mobile phase was switched from methanol to n-hexane, the retention times were shortened. The mobile phase of methanol/n-hexane (70:30 v/v) at a flow rate of 0.2 mL/min produced the best results, with an enantiomer resolution of 0.83. Consequently, further chemical and pharmacological research on nafimidone alcohol and its enantiomers can be facilitated by the proposed HPLC approach.

Key Words: Amylose tris(3,5-dimethyphenylcarbamate), Chiralpak AD, arylalkylazole, nafimidone alcohol.

1 INTRODUCTION

The (arylalkyl)azole structure is shared by the anticonvulsant drugs nafimidone, denzimol, and loreclezole, which lack the ureide structure (Figure 1). One of the most well-known examples of this category is loreclezole, which has a triazole ring as part of its structure. The group's other two members, nafimidone and denzimol, also include an azole group that includes an imidazole ring [1,2].

*Corresponding Author: Zeynep ÖZDEMİR
E-mail: zeynep.bulut@inonu.edu.tr
Submitted: 24.08.2023 Accepted: 11.10.2023

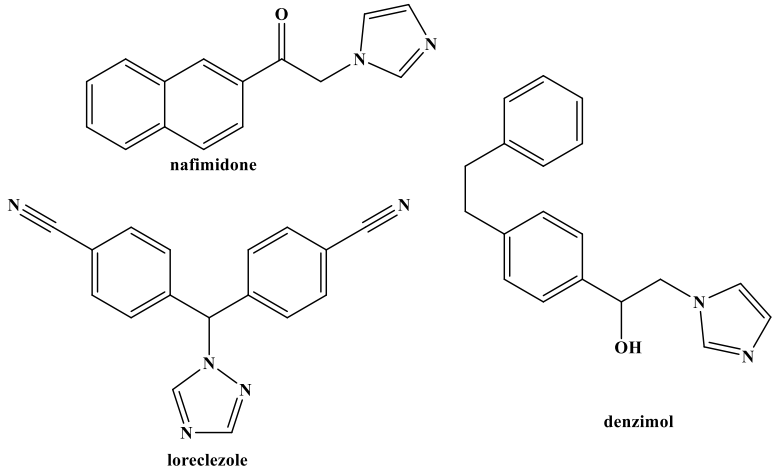

Figure 1. Structure of nafimidone, denzimol and loreclezole.

In contrast to barbiturate and valproic acid, nafimidone and denzimol have an acting profile that is comparable to that of phenytoin and carbamazepine. The main metabolite of nafimidone, nafimidone alcohol, likewise functions as an anticonvulsant (Figure 2) [3,4].

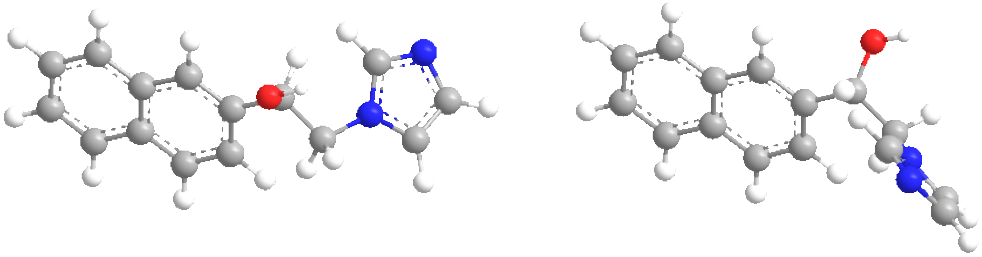

Figure 2. Structure of nafimidone alcohol.

Drug metabolism, also known as biotransformation, is the process by which medications undergo molecular changes within the body after being delivered [5, 6]. Variations in the drug's physicochemical qualities, pharmacological activity, duration of action, and toxicity may arise as a result of chemical changes that metabolic reactions make to the drug's structure. In terms of medication development, metabolism investigations are crucial since they offer crucial information for creating molecules that are more efficient, less toxic, and highly safe. Metabolites are the substances created as a result of metabolic processes. Drug toxicity generally lowers due to metabolism (detoxification), and the compound's removal from the body in water-soluble form is facilitated. Certain medications' biological activity can also be

observed in their metabolites. They are referred to as active metabolites. Occasionally, active metabolites can transform into a structure that has distinct effects [7, 8].

According to reports, the pharmacological properties of several medications' metabolites determine their effects. More efficient molecules were created by synthesizing metabolites after metabolic studies were used to determine the impacts of metabolites [6].

Hepatic microsomes from rats that had previously received phenytoin were used to examine the effects of nafimidone and nafimidone alcohol on the p-hydroxylation of phenytoin. The hydroxylation of phenytoin was inhibited by nafimidone and nafimidone alcohol in a concentration-dependent way at both high-affinity and low-affinity metabolic sites. In doses below micromolar, both substances worked as inhibitors. Both metabolic areas had an inhibitory pattern that was consistent with "mixed-type" inhibition. For nafimidone alcohol, the computed inhibition constants Ki were roughly 0.2 M in both locations. Nafimidone and nafimidone alcohol both prevented carbamazepine epoxidation at submicromolar doses. As a result, it was discovered that nafimidone and nafimidone alcohol are powerful inhibitors of two crucial biotransformation routes [9].

Due to the chiral carbon atom that the nafimidone alcohol molecule bears, it has two enantiomers. The biological, pharmacokinetic, pharmacodynamic, and toxicological characteristics of chiral pharmacological enantiomers can vary [10, 11]. The enantiomers of chiral substances create diastereomeric drug-receptor complexes with chiral receptors, and because the proteins in the organism are likewise chiral, stereoselective activity is seen as a result. It's possible that one of the enantiomers has a therapeutic impact while the other has unfavorable side effects or toxic effects, that one is active while the other is inactive, or that both have various therapeutic effects [12]. Enantiomers can be absorbed, interact with receptors, bind to plasma proteins, undergo biotransformation, and be excreted in stereospecific ways. To examine the pharmacological, pharmacokinetic, pharmacodynamic, and toxicological characteristics of the enantiomers of new biologically active chiral compounds separately, it has become more important in recent years to obtain pure enantiomers and determine the enantiomeric composition of chiral drugs in pharmaceutical analysis [13].

HPLC is frequently used to analyze or prepare enantiomers for separation and to determine the optical purity of each enantiomer. By utilizing chiral mobile phase on non-chiral stationary phase or chiral stationary phase using non-chiral mobile phase, direct enantiomer separation is achieved via chromatographic methods. The separation of racemic substances into their enantiomers has been effectively accomplished in recent years thanks to the development of numerous chiral stationary phases and the utilization of cellulose and amylose derivatives adsorbed on macroporous silica gel [14-17].

The enantiomeric separation studies of 2-(1H-imidazole-1-yl)-1-naphthalene-2-yl)ethanol esters, 1-(naphthalene-2-yl)ethanol esters, and 1-(1-hydroxynaphthalene-2-yl)-2- (1H-imidazole-1-yl)ethanol molecules with anticonvulsant effects have been previously published [18]. The racemic mixture nafimidone alcohol used in this investigation, was analytically separated into its enantiomers by HPLC using various ratios of n-hexane:MeOH solutions as the mobile phase and amylose tris(3,5-dimethylphenylcarbamate) (Chiralpak AD) as stationary phase. Chromatographic information was used to characterize each enantiomer.

2 MATERIAL AND METHOD

Following the procedures described in the literature, the nafimidone alcohol molecule that was isolated in this study was created from 2-acetylnaphthalene [18-21]. In an ice bath, acetic acid was dissolved in 0.05 mol of 2-acetylnaphthalene. A few drops of hydrobromic acid were added to the reaction medium in a three-necked flask, and then, while the mixture was being constantly stirred, 0.05 mol of bromine that had been diluted with acetic acid was added dropwise using a dropping funnel attached to the reaction flask after the bromine was added, the reaction was continued for a further three hours at room temperature while being stirred. At the conclusion of the reaction, the mixed was poured into ice water to solidify it. The precipitate was filtered, then dried in the dark after being cleaned with sodium bicarbonate solution. Crystallization from a methanol/water solution is used to purify the compound (naphthacyl bromide). A solution of 0.03 mol imidazole in 2.5 ml of dimethylformamide that had cooled in an ice bath was gradually mixed with a solution of 0.01 mol naphthacyl bromide in 2.5 ml of dimethylformamide. It was stirred for two hours in an ice bath, then left at room temperature overnight. Ice water was added to the reaction media. The precipitated was filtered and dried. By

crystallization from methanol, it was made pure and nafimidone was occured. 25 ml of methanol and 1.5 mmol of nafimidone were combined, and the mixture was then cooled in an ice bath to 5ºC. The reaction vessel was then filled with 4.5 mmol of sodium borohydride, and it was stirred in an ice bath for an hour. When the methanol was removed from the process, the residual residue was made solid by adding ice water, and it was then refined by crystallization with the aid of the proper solvents to get final compound nafimidone alcohol.

2.1 Enantiomer Separation Studies by HPLC

The chiral separation of the nafimidone alcohol was accomplished using an Agilent 1100 Series High Pressure Liquid Chromatography apparatus, an Agilent Quaternary Pump, and an Agilent Multiple Wavelength Detector. The analyses were conducted at room temperature and at the wavelengths where the compound exhibited the greatest absorption.

For the separation, a chiral column covered with silica gel and made of amylose tris(3,5-dimethylphenylcarbamate) (Chiralpak AD; 25 cm x 4.6 mm inner diameter; particle size 10 m) was utilized by Daicel Chemical Industries, Ltd.

High pressure liquid chromatography solvents were used to create solvent systems with methanol:n-hexane combined in various ratios (100, 90:10, 80:20, and 70:30) as the mobile phase (HPLC purity Merck). In methanol, each chemical was dissolved at a level of roughly 0.5 mg/mL. In accordance with the normal phase mode, analyses were carried out using a Chiralpak AD column at room temperature (22°C). Using an isocratic method, a combination of methanol and n-hexane in varying concentrations was used for the mobile phase elution. Every solvent is HPLC pure. The UV detection wavelength was 254 nm, and the flow rate was adjusted at 0.2 mL min-1. Gallic acid was used to calculate the unretained peak's retention time (t_0). It was employed in subsequent computations and remained constant for each chromatographic run at a fixed flow rate. Average values of duplicate determinations are retention times.

3 RESULTS

On the chiral stationary phase, the molecules amylose tris(3,5-dimethylphenylcarbamate) (Chiralpak AD) were split into their enantiomers (a mixture of methanol and hexane was used as the mobile phase in the ratios specified below) (Table 1).

Table 1. Separation of nafimidone alcohol into its enantiomers on the chiral stationary phase of amylose tris(3,5-dimethylphenylcarbamate) (Chiralpak AD)

Hex (%)	k_1	k_2	α	R_S	N_1	N_2	t_1	t_2
0	0.12	0.18	1.50	0.69	6527	1499	10.10	10.65
10	0.23	0.28	1.23	0.54	7872	1527	12.20	12.70
20	0.39	0.47	1.21	0.74	3660	2166	12.10	12.80
30	0.36	0,44	1.23	0.83	4860	2218	12.20	12.95

Analyzes were performed at λ max, with a flow rate of 0.2 ml/min. n The compound is not separated into its enantiomers. Plots of the retention factors (k_1 and k_2), selectivity (α), resolution factors (R_S) and number of layers (N_1, N_2).

The synthesized chemicals were created as racemic mixes because they had an asymmetric center in their structures. By using a chiral column made of amylose tris(3,5-dimethylphenylcarbamate) (Chiralpak AD) coated on silica gel, enantiomers of the substances were separated by HPLC.

The polysaccharide phenylcarbamate derivative CSP group, which forms the basis of separation using the Chiralpak AD column, is based on the production of the diastereomeric solute-CSP complex. The polar carbamate groups in the CSP structure make hydrogen bonds with the compounds' O- and N-H groups and engage in - interactions via aromatic rings to produce the solute-CSP complex. The solute-CSP complex is stabilized by the presence of aromatic rings in the compounds' structures, and the enantiomers' steric compatibility with this space varies as a result (Figure 3).

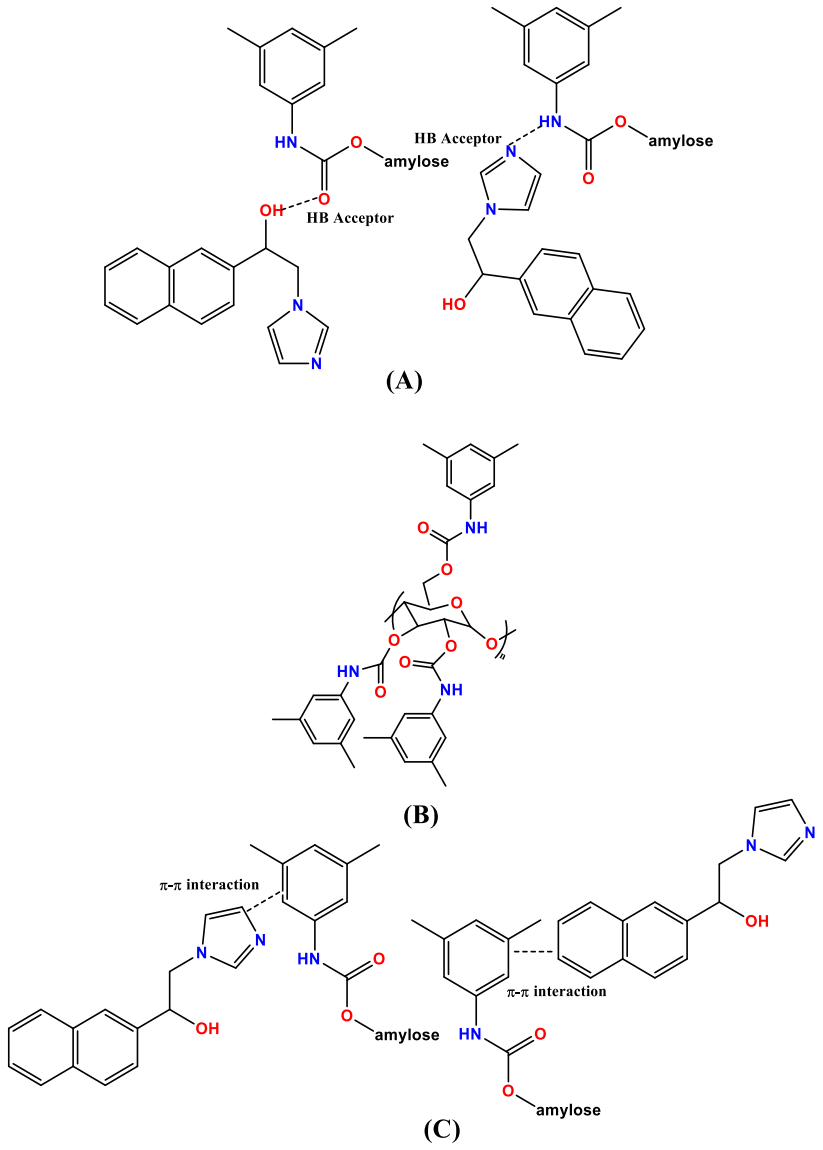

Figure 3. Chemical interactions between synthesized compounds and CSP; (A) proposed interactions of amylose CSP with acceptor hydrogen bonds of compounds, (B) structure of Amylose tris(3,5-dimethylphenylcarbamate, and (C) proposed interactions of π-π-bonds with compounds between amylose CSP [22].

In this research, the chiral separation of the compounds was carried out using methanol:n-hexane mixed mobile phases, which included just methanol and varying concentrations of n-hexane (0–30%). Our chromatographic system is seen within the context of the normal phase mode due to the high methanol content in our mobile phase. The chemical was successfully separated at all ratios, and it was noted that the resolution and selectivity values rose as the hexane ratio rose. Reverse phase HPLC analyses employing C18 columns have also shown the capability of Chiralpak AD columns to perform chiral separation investigations of substances (Figure 4).

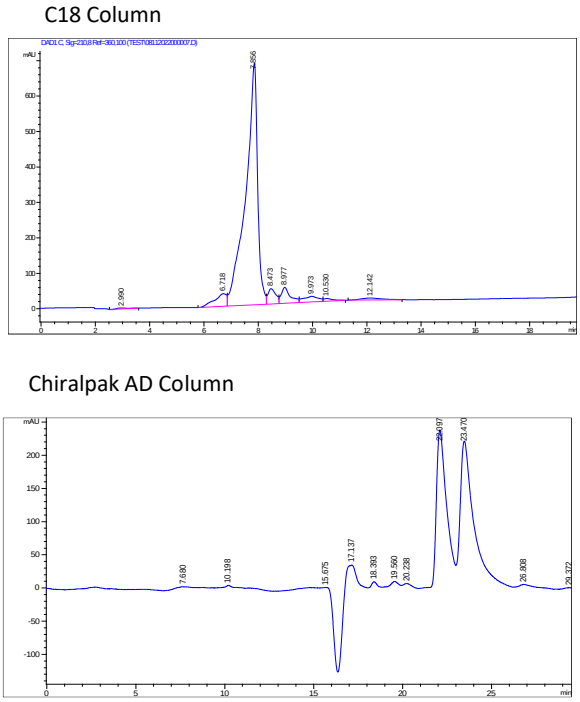

Figure 4. Chromatograms of nafimidone alcohol with C18 column and Chiralpak AD column.

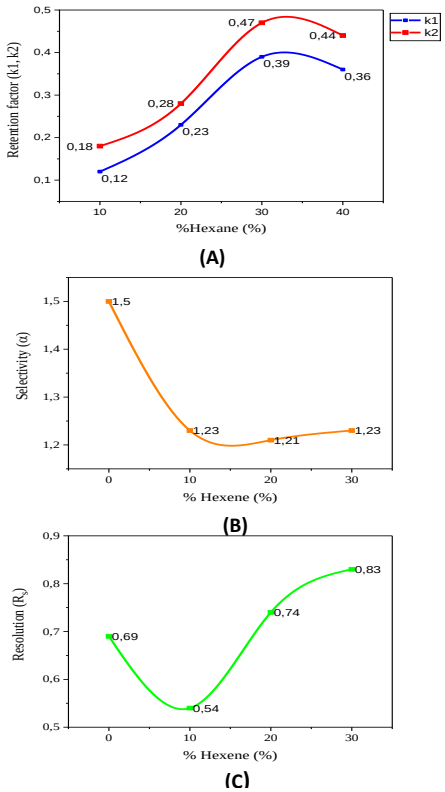

Figure 5. Effect of n-hexane content on retention time (A) k_1: plots of the retention factors for one enantiomer and k_2: plots of the retention factors for one enantiomer, selectivity (B) and resolution (C).

Figure 5's graph illustrates how the amount of n-hexane in the methanol employed as the mobile phase affects retention time, selectivity, and resolution.

4 DISCUSSION

In this study, Chiralpak AD columns were utilized at a flow rate of 0.2 ml/min to analytically separate the enantiomers of the nafimidone alcohol molecule from the arylalkyl azole anticonvulsant drugs using methanol/n-hexane solutions. The composition of the mobile phase had an impact on the chromatographic parameters. The fundamental separations of the compounds under investigation were not visible when methanol and ethanol alone were utilized as the mobile phase, but baseline separations were obtained when methanol/n-hexane combinations were. The methanol/n-hexane (70:30) mobile phase is the most effective for achieving baseline separation in the shortest time. According to the chromatographic results, the analytical HPLC approach created in this study can also be used to prepare the molecule for separation on the Chiralpak AD column in order to determine the pharmacological activity of each enantiomer.

This method development study, which is an early stage of our chiral separation studies, is a step toward the preliminary separations that are planned to take place in the future.

5 ACKNOWLEDGEMENTS

This research did not receive any specific grant from funding agencies in the public, commercial, or not-for-profit sectors.

6 AUTHOR CONTRIBUTIONS

Hypothesis: E.K.K., Z.Ö.; Design: Z.Ö.; Thesis student: E.K.K., Thesis advisor: Z.Ö.; Enantiomer separation studies: E.K.K.; Synthesis of compounds: Y.N.Z., A.K.; Manuscript writing: Z.Ö.

7 CONFLICT OF INTEREST

The authors declare that there is no conflict of interests regarding the publication of this paper.

8 REFERENCES

[1] Nardi D, Tajana A, Leonardi A, Pennini R, Portioli F, Magistretti MJ, Subissi A. Synthesis and anticonvulsant activity of N-(benzoylalkyl)imidazoles and N-(omega-phenyl-omega-hydroxyalkyl)imidazoles. J Med Chem., 1981; 24(6):727-73.

[2] Walker KA, Wallach MB, Hirschfeld DR. 1-(Naphthylalkyl)-1H-

imidazole derivatives, a new class of anticonvulsant agents. J Med Chem., 1981; 24(1):67-74.

[3] Wingrove PB, Wafford KA, Bain C, Whiting PJ. The Modulatory Action of Loreclezole at the Gamma-Aminobutyric-Acid Type-a Receptor Is Determined by a Single Amino-Acid in the Beta-2 and Beta-3 Subunit. P Natl Acad Sci USA., 1994; 91(10):4569-4573.

[4] Graham DJM, Eadie J, Leadbetter BM, Metcalf R. Simultaneous Determination of Nafimidone [1-(2-Naphthoylmethyl)Imidazole], a New Anti-Convulsant Agent, and a Major Metabolite in Plasma by High-Performance Liquid-Chromatography. J Chromatogr., 1983; 275(1):211-216.

[5] Yang L, Li Y, Hong H, Chang CW, Guo LW, Lyn-Cook B, Shi L, Ning B. Sex Differences in the Expression of Drug-Metabolizing and Transporter Genes in Human. Liver J Drug Metab Toxicol., 2012; 3(3):e111.

[6] Özdemir Z, Karakurt A. İlaç Metabolizması ve Farmasötik Kimyada Önemi. Ann. Med. Health Sci. Res. 2016; 5:35-46.

[7] Fura A. Role of pharmacologically active metabolites in drug discovery and development. Drug Disc Today., 2006; 11:133-142.

[8] Das N, Dhanawat M, Dash B, Nagarwal RC, Shrivastava SK. Codrug: An efficient approach for drug optimization. Eur J Pharm Sci., 2010; 41:571-588.

[9] Kapetanovic IM, Kupferberg HJ. Nafimidone, an imidazole anticonvulsant, and its metabolite as potent inhibitors of microsomal metabolism of phenytoin and carbamazepine. Drug Metab. Dispos., 1984; 12(5):560-564.

[10] Brooks WH, Guida WC, Daniel KG. The significance of chirality in drug design and development. Curr Top Med Chem., 2011; 11(7):760-770.

[11] Bahar A, Sönmez Nİ, Vızdıklar C, Aydın V, Akıcı A. The concept of chirality and its association with drug safety: Raditional review. J Lit Pharm Sci., 2022; 11:77-85.

[12] Gal J. The discovery of stereoselectivity at biological receptors arnaldo piutti and the taste of the asparagine enantiomers historyand analysis on the 125th anniversary. Chiralty., 2012; 24: 959-976.

[13] FDA-US Food and Drug Administration (2022, 4 Nov). Development of new stereoisomeric drugs. https://www.fda.gov/regulatory-information/search-fda-guidance-

documents/development-new-stereoisomeric-drug.

[14] Ye X, Liu Y, Li F. Biomarkers of oxidative stress in the assessment of enantioselective toxicity of chiral pesticides. Curr Protein Pept Sci., 2017; 18:33-40.

[15] Zhang ZH, Xie SM, Yuan LM. Recent progress in the development of chiral stationary phases for high-performance liquid chromatography. J Sep Sci., 2022; 45:51-77.

[16] Remelli M. Chiral ligand–exchange chromatography of pharmaceutical compounds on dynamically coated(home-made) stationary phases. Curr Med Chem., 2017; 24:818-828.

[17] Fernandes C, Carraro ML, Riberio J, Araujo J, Tititan ME, Pinto MM. Synthetic chiral derivatives of xanthones: Biological activities and enantioselectivity studies. Molecules., 2019; 24:791.

[18] Karakurt A, Saraç S, Dalkara S. Enantioseparation of some new 1-(2-naphthyl)-1-ethanol ester derivatives by HPLC on Chiralcel OD, Chromatographia., 2012; 75(19-20):1191-1197.

[19] Sarı S, Akkaya D, Zengin M, Sabuncuoğlu S, Özdemir Z, Alagöz MA, Karakurt A, Barut B. Antifungal azole derivatives featuring naphthalene prove potent and competitive cholinesterase ınhibitors with potential cns penetration according to the in vitro and in silico studies. Chem Biodiversity., 2022; 19:27.

[20] Bozbey İ, Uslu H, Türkmenoğlu B, Özdemir Z, Karakurt A, Levent S. Conventional and microwave prompted synthesis of aryl(alkyl)azole oximes, 1H-NMR spectroscopic determination of E/Z isomer ratio and homo-lumo analysis. J Mol Struct., 2022; 1251:1-12.

[21] Karakurt A, Bozbey I, Uslu H, Sarı S, Özdemir Z, Şalva E. Synthesis and cytotoxicity studies on new pyrazole-containing oxime ester derivatives. Trop J Pharm Res., 2019; 18:1315-1322.

[22] Gambacorta N, Özdemir Z, Doğan İS, Ciriaco F, Zenni YN, Karakurt A, Saraç S, Nicolotti O. Integrated experimental and theoretical approaches to investigate the molecular mechanisms of the enantioseparation of chiral anticonvulsant and antifungal compounds. J Mol Struct., 2022; 1270, 133905.

e-ISSN: 2980-0463
Anat. J. Pharm. Sci 2023:2(1)
AJPS
Research Article

Structural and Functional Impacts of the Altered Hydrophobicity in the Dimer Interface of *Tpv* HSP 14.3

Sema ZABCI[1*], Azra RAFIQ[2], Semra KOCABIYIK[1]

[1]Middle East Technical University, Faculty of Art and Science, Department of Biological Sciences, 06800, Ankara, Türkiye

[2]Riphah International University, Faculty of Pharmacy, Department of Pharmaceutical Sciences, 54000, Lahore, Pakistan

ABSTRACT: Small heat shock proteins (sHSPs) are the ATP-independent molecular chaperones that prevent protein aggregation in the cell by forming stable complexes with unfolded and misfolded proteins. Their distinctive structural characteristics are their low molecular weight (from 14 to 43 kDa) and a tripartite domain architecture. The highly conserved Alpha Crystallin Domain (ACD) plays a central role in the dimerization of sHSPs and acts as the structural building block for oligomerization. The point mutations in the ACD of the human sHSPs that interfere with the dimer integrity are linked to several diseases, including cataracts, desmin-related myopathy, cardiomyopathy, and distal hereditary motor neuropathy. In the present study, we investigated the functional and structural implications of amino acid changes at two putative dimer interface residues, L33 and Y34. These residues are located on the β2 strand of *Tpv* HSP 14.3, which is implicated in ACD dimerization via strand exchange. Effects of the substitutions were evaluated by performing chaperone assays using the client proteins pig heart Citrate Synthase (phCS) and Alcohol Dehydrogenase (ADH) and through *in silico* molecular bond and structure analyses of the wild type and generated mutant proteins. Our results indicated that an excess amount of WT and the mutant proteins are required to maintain phCS activity to a level comparable to or even higher than the positive control. At a lower substrate/sHSP ratio, the Y34F mutant protected the phCS activity more effectively than the WT and L33S mutant sHSPs. Also, the Y34F mutant sHSP afforded the highest protection of ADH enzyme from heat inactivation. It is likely that increased hydrophobicity by Y34F substitution contributed to the formation of a hydrophobic surface that may capture aggregation-prone substrates. According to molecular bond analysis, the loss of intermolecular hydrophobic interactions between leucine 33 on the β2 strand and tyrosine 77 and isoleucine 78 on the β6 strand can be critical for the reduced structural/thermodynamic stability of the L33S mutant protein.

Keywords: *Thermoplasma volcanium*, small heat shock protein (sHSP), site-directed mutagenesis, dimer interface, alpha crystallin domain, 3-D structure analysis.

*Corresponding Author: Sema ZABCI
E-mail: sema.zabc@yahoo.com
Submitted: 23.11.2023 Accepted: 02.12.2023

1 INTRODUCTION

Small heat shock proteins (sHSPs) are the ATP-independent molecular chaperones that play essential roles in maintaining protein homeostasis in the cells [1]. The sHSPs are constitutively expressed to prevent protein aggregation, and their expression level is immediately induced upon exposure to stress factors (*e.g.*, heat, oxidative, and pH stress) [2]. They form stable complexes with denaturing proteins and sequester them in a folding-competent state. Substrate release and subsequent refolding are achieved through the participation of ATP-dependent chaperones such as Hsp70 and Hsp100 [3]. The sHSPs are present in three kingdoms of life and some viruses. The low molecular weight (*i.e.*, 12 to 43 kDa) and a tripartite domain architecture are their characteristic structural features [4]. The unique central element α-crystallin domain (ACD) is highly conserved and composed of seven to eight β-sheets that adopt an immunoglobulin fold. The ACD (consists of 90–100 amino acids) is flanked by variable and flexible N-terminal domain (NTD) and C-terminal domain (CTD) [5]. The ACD plays an important role in the dimerization of sHSP, and the ACD dimer is the basic building unit for the subsequent oligomerization of small heat shock proteins [6, 7]. There are two types of defined dimerization modes. In non-metazoans (archaeal, bacterial, yeast, and plant), a symmetric dimer is formed by strand exchange in the ACD of sHSPs so that the β6 strand of one ACD interacts with the β2 strand of the partnering ACD. In metazoan sHSPs, the extended β6-β7 strands of the partnering ACDs are linked through ionic and hydrophobic interactions and hydrogen bonds, leading to the formation of the ACD dimer [8, 9]. Starting from the ACD dimer, the formation of higher-order oligomers (12 to > 48 subunits) involves a hierarchy of interactions by the participation of NTE and CTE elements [10, 11]. The highly polydisperse oligomeric forms of sHSPs are dynamic and can dissociate into smaller species, predominantly dimers, as a response to changes in conditions such as temperature and pH or modifications such as phosphorylation. This dynamic feature is crucial for the chaperone function of sHSPs [12].

The interaction between the two sheets of the ACD dimer is relatively weak, with a dissociation constant in the order of a few micromolar [13]. There are several reports indicating that disruption of the dimer interface in human sHSPs by mutations, which are diseases associated, had significant effects on the structure and

function of the sHSPs by blocking subunit exchange [14]. Among such mutations, there are cataract associated R116C mutation of αA-crystallin, desmin related myopathy and cardiomyopathy associated R120G mutation of αB-crystallin, and distal hereditary motor neuropathy related K141E mutation of HSP22 [14–18]. The equivalent of these residues is arginine 107 in the archaea *Methanocaldococcus jannaschii* (Mj) Hsp 16.5, and the R107G substitution resulted in the formation of larger and more polydisperse oligomers than the wild type MjHsp16.5 [19]. Except this, there is not any report on the investigation of the dimer interface interactions by targeting specific residues in archaeal sHSPs.

In this study, we aimed to fill the gaps in the literature concerning the role of hydrophobicity in the dimer interface of sHSPs. In our experiments, we specifically targeted two residues, L33 and Y34, of the *Tpv* HSP 14.3, which are predicted as putative interface residues by the NCBI Conserved Domain Database search. These residues are located on the β2 strand, which is directly involved in dimerization by interconnecting with the β6 loop. The hydrophobicity of the dimer interface was altered by site-specific mutagenesis. Chaperone activity assays and *in silico* molecular bond and structure analyses of the wild type and mutant proteins were performed in comparison with the wild types.

2 MATERIAL AND METHOD

2.1 Recombinant Plasmid Construction

The recombinant *Tpv* HSP 14.3 gene encoding Hsp20/alpha crystallin family protein (locus name TVG_RS04180, sequences 790978..791352) of *Thermoplasma volcanium* [20] was cloned into the expression vector pET21a (+) (Novagen, Madison, WI) following the Kit protocol. The *Tpv* HSP 14.3 gene from the plasmid pDrive-tpv14.3 was amplified by PCR (Gene Cycler, Techne Inc., NJ, USA) using the forward primer (5'-TGAGCATATGTATACACCCATAAAG TTCTTTACG-3') with *Nde*I recognition site and the reverse primer (5'-TGAGGGATCCCACCCAATCACATCA AGCATAC-3') with *Bam*HI recognition site. After purification (QIAquick Gel Extraction Kit, QIAGEN Inc., Valencia, USA), the amplified gene was introduced into the expression vector pET21a (+) at *Nde*I and *Bam*HI sites using DNA Ligation Kit (Novagen, Madison, WI). Putative recombinant plasmids were transferred into chemically competent *E.coli* BL21 (DE3) cells (New England Biolabs, Ipswich, Massachusetts) by transformation. The sequences of the plasmids from selected

recombinant clones were confirmed by DNA sequencing (Oligomer Company, Ankara, Türkiye). One of the verified expression constructs carrying the *Tpv* HSP 14.3 gene was named pET21_tvsHSP2 and transformed into *E.coli* BL21 (DE3) cells (New England Biolabs, Ipswich, Massachusetts) for expression of the wild type sHSP.

2.2 Site-Directed Mutagenesis

Single amino acid substitution (L33S and Y34F) mutants of the *Tpv* HSP 14.3 were generated by PCR-mediated mutagenesis using Quick-Change II Site-Directed Mutagenesis Kit (Agilent Technologies Inc. Santa Clara, California, USA). The mutagenic oligonucleotide primer pairs that were designed according to Kit's instructions are given in Table 1. The recombinant plasmid pET21_tvsHSP2 with cloned *Tpv* HSP 14.3 gene was used as the template in the mutagenesis experiments. The mutations were verified by DNA sequencing (Genscript Biotech, Piscataway, New Jersey, USA). For high efficiency protein expression, mutant plasmid constructs were transformed into competent *Escherichia coli* BL21(DE3) cells.

Table 1. List of the mutagenic oligonucleotide forward (f) and reverse (r) primers

Mutation	Sequence of the Mutagenic Oligonucleotide Primers
L33S-f	5'-cca ccagtcacg**tca** tat caa gat agc-3'
L33S-r	5'-ctatcttgata**tga**cgtgactggtgg-3'
Y34F-f	5'-cca ccagtcacgtta**ttt**caa gat agc tct-3'
Y34F-r	5'-agagctatcttg**aaa**taacgtgactggtgg-3'

2.3 Protein Expression and Purification

The cell lysates were prepared mainly according to the pET System Manual Instructions. Overnight cultures of wild type and mutant *E.coli* BL21(DE3) strains were grown at 37ºC in Luria-Bertani (LB) medium containing ampicillin (100 µg/mL) with vigorous shaking to an OD_{600} of 0.5-0.7. Overexpression was induced by adding isopropyl thio-β-D-galactoside (IPTG) to a final concentration of 1 mM. The growth was continued for 4-5 hours before cells were harvested by centrifugation at 5000 x g for 20 min at 4ºC (JOUAN SA, Herblain-France). The cell pellet was resuspended in 10 mL lysis buffer (25 mM Tris, 1 mM EDTA, 30 mM NaCl pH 7.5). The cells were broken by sonication (Sonics and Materials, USA), and supernatants of the lysates were obtained by centrifugation at 20000 xg for 20 min at 4ºC (Sigma 3K30 Centrifuge, Sigma Chemical Co., USA). The supernatant fraction containing soluble sHSP was heated between 60°C and 80°C

to investigate the expressed protein's heat stability. The denatured protein was removed by centrifugation at 12000 xg for 1 hour at 4ºC. The cleared lysate was stored at -20ºC until use.

SDS polyacrylamide gel electrophoresis (SDS-PAGE) was used to analyze the progress of the expression. For purification, the soluble protein fractions were applied to a pre-packed anion exchange HiTrap Q column (Amersham Biosciences, U.S.A.), connected to the AKTA prime HPLC system (Amersham Biosciences, U.S.A.). The bound proteins were eluted at a flow rate of 5.0 mL/min with a linear gradient of NaCl (0-1 M) in the start buffer (20 mM Tris, pH 8.41). Peak fractions containing *Tpv* HSP 14.3 as deduced by SDS-PAGE gel and OD280 measurements (Picopet 01, Picodrop Ltd. U.K.), were pooled, concentrated, and desalted by ultracentrifugation (Vivaspin 5 kDa cut-off, Sartorius, Germany). Purity was checked by SDS-PAGE.

2.4 Chaperone Activity Assays

Chaperone activities of the *Tpv* HSP 14.3 and mutant variants were characterized as the ability to protect the client proteins pig heart Citrate Synthase (phCS) (EC 4.1.3.7, Sigma) and Alcohol Dehydrogenase (ADH) (EC 1.1.1.1, Sigma) from heat-induced inactivation, as described previously [20, 21].

phCS heat protection assay was performed by pre-incubating the enzyme at 47°C for 10 min in the presence or absence of the sHSP. Then, the remaining CS activity was measured at 35°C by continuously monitoring the absorbance at 412 nm (Shimadzu UV-1601A, Kyoto, Japan). The protection effect of *Tpv* HSP 14.3 was evaluated at three substrate/sHSP, w/w ratios of 1:500, 1:250, and 1:147.

For the ADH heat protection assay, the enzyme was pre-heated at 47°C for 20 minutes, with or without *Tpv* HSP 14.3 protein at an ADH/chaperone (w/w) ratio of 1:90. The ADH activity was measured by continuously recording the rate of NAD^+ reduction spectrophotometrically at 340 nm [21].

Each experiment was repeated at least three times. The data analysis and plotting of the graphics were achieved by using GraphPad Prism 9.0 software (GraphPad, USA).

2.5 Bioinformatics and 3-D Structure Analysis

The multiple alignments (MSA) were performed by the Clustal W Program in the EMBL-EBI database (https://www.ebi.ac.uk/Tools/msa/clustalo/). The secondary structure features incorporated into the MSA were obtained by the Jalview [22]. Putative dimer interface residues were predicted by Conserved Domain Database (CCD) search (National

Center for Biotechnology Information, https://www.ncbi.nlm.nih.gov/cdd/). The homology model of the *Tpv* HSP 14.3 3-D structure was generated by MODELLER 9.15 Ver server. Crystal structures of *Xanthomonas axonopodis* (PDB entry 3GLA), *Sulfolobus tokodaii* (PDB entry 3AAC and 3VQM), and *Deinococcus radiodurans* (PDB entry 4FEI) were used as templates. Visualization, energy minimization, and structure analyses of the models were achieved using the UCSF Chimera Program. The BIOVIA Discovery Studio Visualizer (DSV) (Ver 4.5) was used for the analysis of the weak molecular interactions in the generated 3-D models. Thermodynamic stability analysis of the *Tpv* HSP 14.3 proteins was performed using the MUpro web server [23].

3 RESULT

3.1 Multi-Sequence Alignment of ACD Sequences of *Tpv* HSP 14.3 and Other Representative Archaeal sHSPs

Multiple sequence alignment of the ACD sequences of the archaeal sHSPs showed that highly conserved residues were found in the core alpha-crystallin domain spanning residues L33-K114 in *Tpv* HSP 14.3. The similarity scores range from 52.7 % to 90.2 % within the total 82 amino acid ACD sequence. The ACD is composed of eight beta strands named from β2 to β9 (Figure 1). The residues we targeted for mutagenesis, L33 and Y34, are predicted as two of the residues forming the monomer-monomer interface. These amino acids reside on the β2 strand, which is involved in dimerization by interacting with the β6 strand of the partner monomer. The equivalent residues at position 33 are all hydrophobic residues *i.e.*, methionine or isoleucine. This may indicate the importance of hydrophobicity at this position and its possible involvement in hydrophobic interaction in the dimer interface. The tyrosine at position 34 is also highly conserved, except the sHSPs of hyperthermophilic archaea, *Pyrococcus furious* and *Thermococcus kodakarensis,* where F exists at the corresponding position. The common feature of these amino acids is their aromatic side chains.

3.2 Heat Stability of *Tpv* HSP 14.3 Wild Type and ACD Mutants

Before and after heating, when the cell lysates of the wild type (WT) and mutant *Tpv* HSP 14.3 proteins were separated into soluble and insoluble (pellet) fractions by centrifugation and analyzed by SDS PAGE, a significant amount of all sHSPs was recovered in the soluble fraction (Figure 2, Lane1). However, the sHSP was absent in the cell lysate of the *E.coli* BL21(DE3) cells without *Tpv* HSP 14.3 plasmid (negative control), since the sHSP-specific band was not detected on the gel. These results

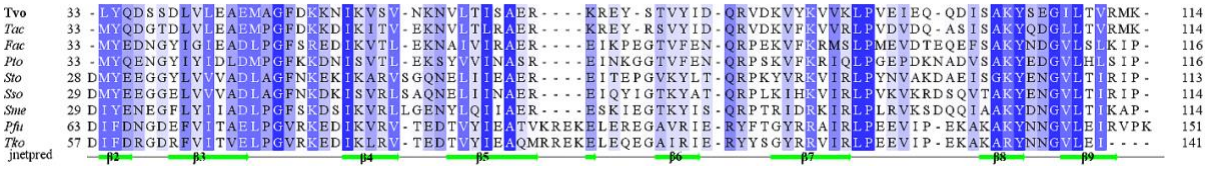

Figure 1. Multiple sequence alignment of alpha crystallin domain of *Tpv* HSP 14.3 with the sHSPs from other archaea. The species names and accession number of their sHSPs are: Tvo; *Thermoplasma volcanium* (CBY78065.1: GSS1), Tac; *Thermoplasma acidophilum* (CAC11993.1: DSM 1728), Fac; *Ferroplasma acidiphilum* (ARD84221.1: Y), Pto; *Picrophilus torridus (*AAT43324: DSM 9790), Sto; *Sulfurisphaera tokodaii* (WP_010979712.1: Str.7), Sso; *Saccharolobus solfataricus* (WP_009989320.1: P2), Sme; *Sulfuracidifex metallicus* (WP_054838418.1, DSM 6482), Pfu; *Pyrococcus furiosus* (AAF71367.1: DSM 3638), Tko; *Thermococcus kodakarensis* (WP_048053707.1: KOD1). Highly conserved residues are shaded by dark blue. Secondary structural features of the ACD are indicated below the alignment. The β strands from β2 through β9 are underlined by green arrows.

indicated the successful expression of recombinant WT and mutant proteins and the effectiveness of the IPTG induction for overexpression (Figure 2b). The L33S and Y34F substitutions produced mutant proteins, which are stable at temperatures up to 70°C (Figure 2b and 2c). Above this temperature (80°C), the sHSP bands, particularly that of the L33S protein, were hardly detectable in the cell lysates of the mutant proteins.

3.3 Functional Characterization of the *Tpv* HSP 14.3 WT and Mutant Proteins

To assess the chaperone functions of sHSP proteins, the WT and mutant proteins were compared for their ability to protect the client proteins phCS and ADH from denaturation during heating at 47°C as described in the Material and Methods.

Our results showed that when heated in the absence of sHSP, the phCS activity decreased about 11-fold, so that only 8% of the activity could be recovered (Figure 3). Heat protection efficiency of the WT and mutant sHSPs appeared to be concentration dependent, increasing with increased substrate/sHSP w/w ratio. At a 1:147 CS/sHSP (w/w) ratio, all sHSP variants provided almost equal protection of the phCS activity from heat inactivation. Only

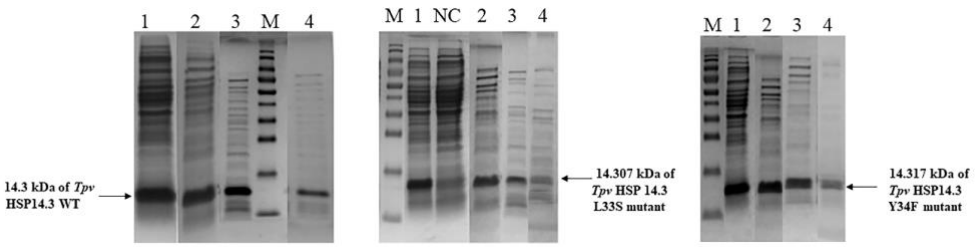

Figure 2. SDS PAGE analysis of wild type *Tpv* HSP 14.3 and its variants before and after heat treatment. a) WT *Tpv* HSP 14.3 b) L33S *Tpv* HSP 14.3 c) Y34F *Tpv* HSP 14.3 M: Page Ruler Pre-Stained Protein Ladder (SM0671, Fermentas). NC: Negative Control. Lane 1: Cell free extract of the *Tpv* HSP 14.3 before heat treatment (BH), Lane 2-4: Heat treatment at 60ºC, 70ºC, and 80ºC, respectively.

~ 30% protection of CS activity could be supported at this substrate/sHSP ratio. At the 1:250 phCS/sHSP (w/w) ratio, the WT and L33S mutant sHSPs achieved ~50% protection of the CS enzyme activity, while Y34F supported relatively higher protection (~67%). At the 1:500 CS/ sHSP (w/w) ratio, the WT sHSP fully protected the CS activity. Remarkably, at the same substrate/sHSP ratio, L33S and Y34F mutants afforded a notable increase (additional 8 to 9 % protection) in the CS activity as compared to WT sHSP.

These results indicated that an excess amount of WT and the mutant proteins are required to maintain CS activity to a level comparable to or even higher than the PC. At lower substrate/sHSP ratio, Y34F sHSP protected the CS activity more effectively than the WT and L33S mutant sHSPs.

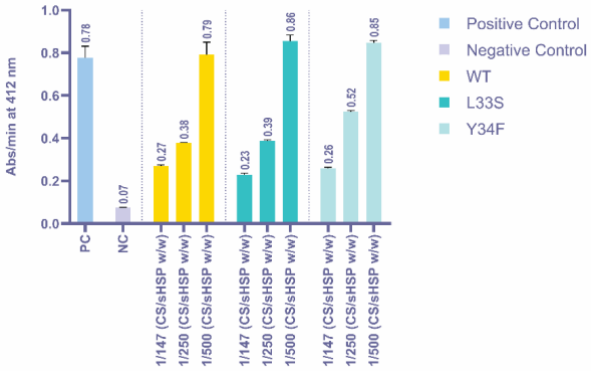

Figure 3. Effect of *Tpv* HSP 14.3 wild type and its mutants on the prevention of CS from thermal inactivation at different CS/sHSP ratios (w/w). After heating at 47°C for 10 min, the remaining activity was assessed by continuously monitoring absorbance at 412 nm. The initial rate of the reaction was calculated as the slope of the increase in absorption. PC: Positive Control, activity measured before heat treatment. NC: Negative Control, remaining activity after heat treatment without the presence of a chaperone. The presented data represent mean values with standard deviation (at the top of each bar) based on a minimum of three independent experiments.

To extend our investigation of the capacity of *Tpv* HSP 14.3 wild type and mutant variant proteins to protect the substrate proteins from heat, we have tested their chaperone activities against thermal inactivation of the ADH enzyme at a 1/90 substrate/ sHSP (w/w) ratio. The enzyme activity assay revealed that heating the enzyme at 47ºC for 20 minutes in the absence of *Tpv* HSP 14.3 (negative control) resulted in a dramatic decrease (~95%) in the ADH activity (Figure 4). However, in the presence of *Tpv* HSP 14.3 WT, 64% of the ADH activity was recovered as compared to the negative control. The chaperone activities of the mutant sHSPs were better than the WT sHSP and about 75% and 87 % of the initial ADH activity was protected by L33S and Y34F mutant sHSP, respectively.

Thus, it is evident from our experiments that the Y34F mutant sHSP has a greater ability compared with other sHSP variants to protect the ADH and phCS from heat inactivation.

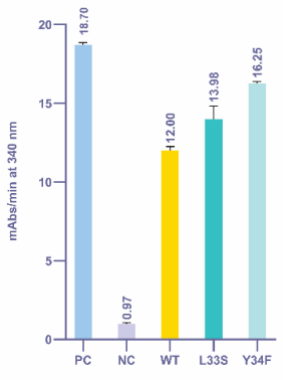

Figure 4. ADH activity assay in the absence and presence of *Tpv* HSP 14.3. The ADH was heated at 47°C for 20 min in the presence or absence of the chaperone. The rate of reduction of NAD^+ was measured at 340 nm. The rate of the reaction was found by analyzing the slope of the initial increase in absorption. PC: Positive Control, activity measured before heat treatment. NC: Negative Control, remaining activity after heat treatment without the presence of a chaperone. The presented data represent mean values with standard deviation (at the top of each bar) based on a minimum of three independent experiments.

3.4 3-D Structure Analysis of *Tpv* HSP 14.3 and its Molecular Interactions

The 3-D structure of *Thermoplasma volcanium* HSP 14.3 was generated by homology modelling. The ACD of *Tpv* HSP 14.3 is like an immunoglobulin fold consisting of two anti-parallel layers such that β2, β3, β8, β9 form one layer and β4, β5, and β7 together with a distinct β6 for the other sheet. A large β6 loop protrudes from

an additional β strand between β5 and β7, which is absent in the ACD of vertebrate sHSPs. This loop is positioned close to the β2 strand of the adjacent monomer and directly involved in ACD dimer formation *via* strand exchange, which is typical for the non-metazoan sHSPs [6]. This core ACD is flanked by an N-terminal region that shows an α-helical structure and an unstructured C-terminal domain (Figure 5).

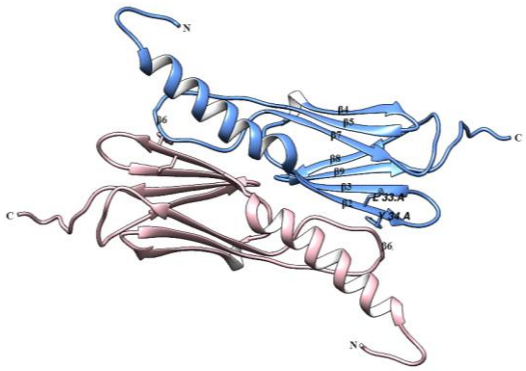

Figure 5. The model structure of *Tpv* HSP 14.3. Interacting monomers of the *Tpv* HSP 14.3 dimer are shown as ribbon diagrams (blue and pink). For clarity, strands β2 to β9 are labeled for only one monomer (colored blue). The L33 and Y34 residues are also indicated on the β2 strand.

The changes in the hydrophobicity characteristics of the ACD dimer surface by amino acid substitutions could be recognized by molecular surface analysis of the 3-D model structures by the CHIMERA program. This program colors the molecular surface according to the hydrophobicity amino acid, ranging from Dodger Blue to red, representing the minimum and maximum values on the Kyte-Doolittle scale.

To understand how the introduced mutations affected the surface properties, 3-D hydrophobicity surface models of *Tpv* HSP 14.3 WT and the mutants were generated. The L33S mutation at this position changed color from red to blue, signifying a reduction in surface hydrophobicity by the introduction of the polar residue serine for the very hydrophobic leucine. On the other hand, the replacement of the tyrosine at position 34 with the highly hydrophobic amino acid phenylalanine enhanced surface hydrophobicity relative to the WT, which is evident from the blue-to-red transition at this position (Figure 6).

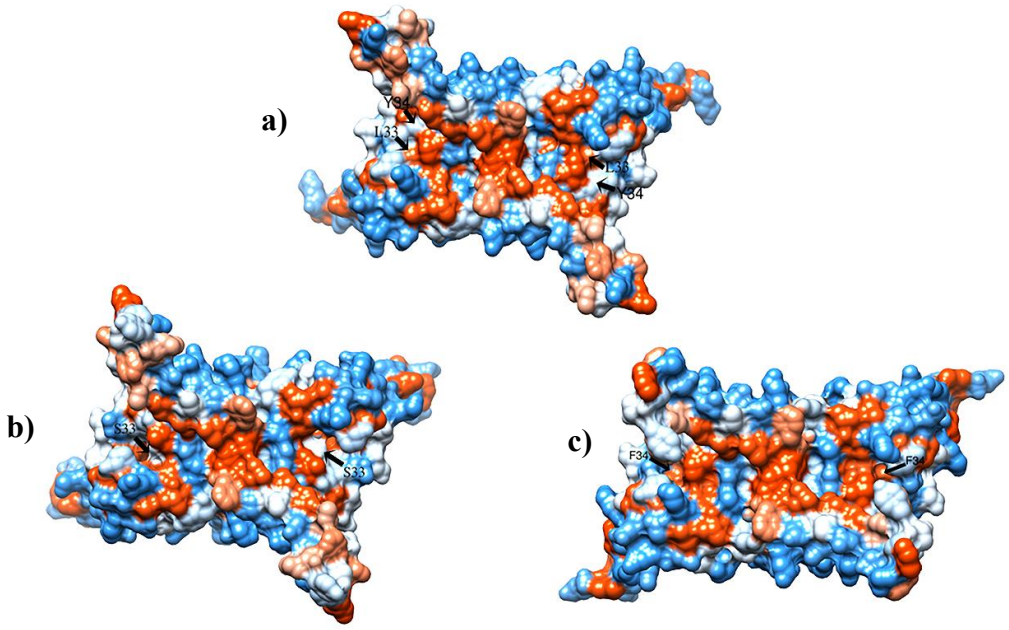

Figure 6. Surface hydrophobicity analysis of *Tpv* HSP 14.3 and its ACD mutants. a) *Tpv* HSP 14.3 WT, b) L33S mutant, c) Y34F mutant. The arrows show the locations of the targeted mutations in which surface hydrophobicity is changed relative to the WT. Min and max values are associated with bright blue and orange-red, respectively.

Comparative analysis of the intra/intermolecular bonds after point mutations was performed by the DSV Program. As a result of the replacement of the hydrophobic amino acid leucine with the polar amino acid serine at position 33 (L33S) resulted in the loss of intramolecular hydrophobic bonds of Leu33-Leu42 and the intermolecular hydrophobic bonds of Leu33-Ile78 and Tyr77-Leu33 (Table 2, Figure 7). The intramolecular hydrogen bonds of the monomers remained unchanged in the L33S protein. Besides two intermolecular hydrogen bonds that are available in the WT sHSP, the L33S mutation formed an additional one between the nitrogen atom of Ile78 and the oxygen atom of Ser33. Moreover, the decrease in the hydrogen bond distance was remarkable, particularly those involved in intermolecular interactions (Table 2). On the other hand, substituting tyrosine with the highly hydrophobic phenylalanine at position 34 by Y34F mutation did not result in any apparent changes in the predicted intramolecular hydrogen and intramolecular hydrophobic interactions (Figure 8). However, it caused alterations in the distances between these bonds, as indicated in Table 3.

Table 2. Intermolecular and intramolecular bond analysis of L33S mutant sHSP as compared with the WT sHSP

Hydrogen Bond in WT	Distance	Hydrophobic interactions in WT	Distance	Hydrogen Bond in L33S	Distance
Intramolecular Interactions				**Intramolecular Interactions**	
B:LEU33:CA - B:VAL41:O	3,3591	A:LEU33 - A:LEU42	4,6659	B:SER33:CA - B:VAL41:O	3,1639
A:LEU33:CA - A:VAL41:O	3,35931	B:LEU33 - B:LEU42	4,6663	A:SER33:CA - A:VAL41:O	3,1639
Intermolecular Interactions				**Intermolecular Interactions**	
B:LEU33:N - A:ILE78:O	3,0712	A:LEU33 - B:ILE78	5,1210	B:SER33:N - A:ILE78:O	2,8393
B:ILE78:N - A:LEU33:O	3,0231	A:ILE78 - B:LEU33	4,6994	B:ILE78:N - A:SER33:O	2,6742
		A:TYR77 - B:LEU33	5,4574	A:ILE78:N - B:SER33:O	2,0301

Table 3. Intramolecular bond analysis of Y34F mutant sHSP as compared with the WT sHSP

Hydrogen Bond in WT	Distance	Hydrophobic interactions in WT	Distance	Hydrogen Bond in Y34F	Distance	Hydrophobic interactions in Y34F	Distance
Intramolecular Interactions				**Intramolecular Interactions**			
B:TYR34:N- B:VAL41:O	3,12704	A:TYR34- A:VAL41	4,03417	B:PHE34:N-B:VAL41:O	3,0023	B:VAL41:CB- B:PHE34	3,8605
B:VAL41:N- B:TYR34:O	2,98035	B:TYR34- B:VAL41	4,03407	B:VAL41:N-B:PHE34:O	3,0042	A:VAL41:CB- A:PHE34	3,8610
A:TYR34:N- A:VAL41:O	3,12661			A:PHE34:N-A:VAL41:O	3,0017		
A:VAL41:N- A:TYR34:O	2,97915			A:VAL41:N- A:PHE34:O	3,0049		

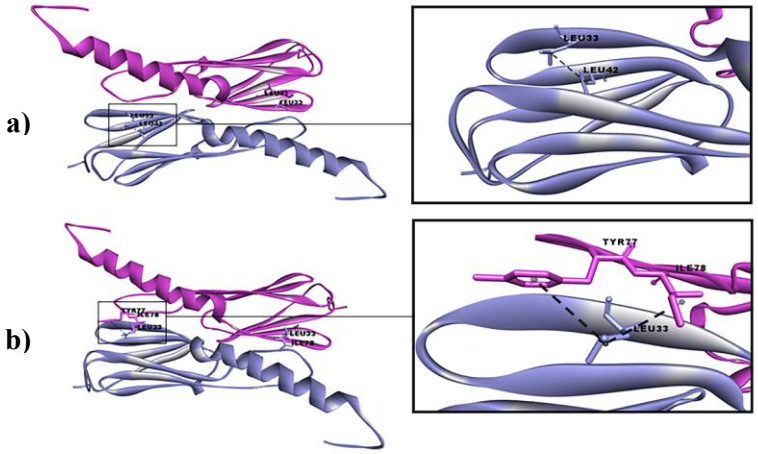

Figure 7. Intra (a) and intermolecular (b) hydrophobic bonds of *Tpv* HSP 14.3 WT at residue Leu33. Pink indicates the one monomer and blue indicates the partner monomer.

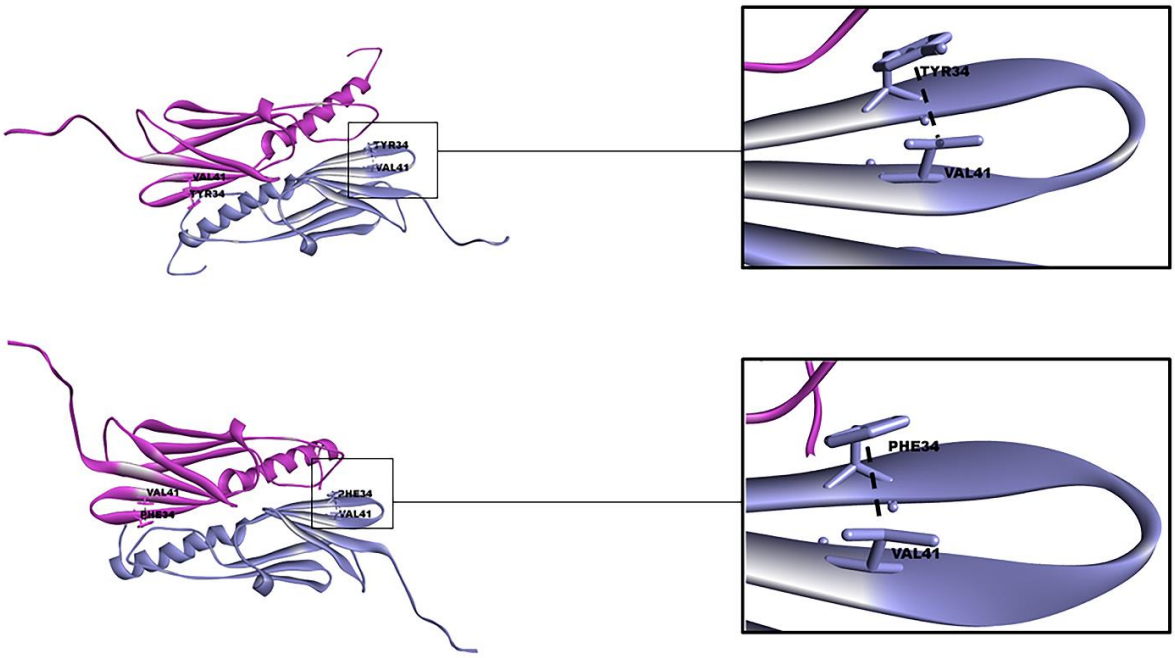

Figure 8. Intramolecular hydrophobic bonds of *Tpv* HSP 14.3 WT (a) and Y34F mutant (b) at residue 34. Pink indicates the one monomer and blue indicates the partner monomer.

3.5 Thermodynamic Stability Analysis of *Tpv* HSP 14.3 Mutants

The stability of proteins is a critical feature that affects their proper functioning, activity, and regulation. Protein thermodynamic stability is quantified by ΔG, which is equal to the difference between the free energy of folded and unfolded states [24]. In order to predict the thermodynamic stability of the mutant sHSPs, we used the MUpro web server. When the relative stability change (ΔΔG), which is the difference between the free energy of wild type protein and mutant proteins, is positive, it indicates that the mutation increases stability and vice versa. The method relies on a confidence score between -1 to 1. A score less than 0 is attributed to the reduced stability after mutation [23]. According to the MUpro analysis, the thermodynamic stability of *Tpv* HSP 14.3 ACD mutants decreased. The L33S mutant (ΔΔG=- 2.203) was apparently less stable as compared to the Y34F mutant (ΔΔG= - 0.41).

4 DISCUSSION

Identifying residues crucial for the ACD dimerization has been documented so far through crystallographic analysis of the sHSP structures from a limited number of species [11, 25–28]. Also, this issue has remained poorly explored experimentally by mutagenesis in archaeal sHSPs. Our research

has focused on two putative interface residues, L33 and Y34, located on the β2 strand of the *Tpv* HSP 14.3, which is involved in ACD dimerization *via* strand exchange, to investigate the functional and structural consequences of these targeted amino acid substitutions.

Our results indicated that *Tpv* HSP 14.3 WT and its two mutant variants, were unaffected from exposure to high temperatures up to 70°C, as deduced by SDS-PAGE analysis. Above this temperature, although there has been a detectable decrease in the solubility of the L33S mutant sHSP relative to WT sHSP, a slight decrease in solubilization of the Y34F mutant protein was observed. Further assessment of the thermodynamic stability by MUpro analysis also suggested that the decline in the thermodynamic stability of the sHSP protein was more pronounced with the L33 to S exchange than with the Y34 to F substitution. It was observed that each hydrogen bond distance in L33S changed remarkably as compared to the WT sHSP. As previously reported, a change in hydrogen bond distance may cause loss of thermodynamic stability as well as aberrant folding and aggregation of the proteins [29, 30]. In addition, the loss of intermolecular hydrophobic interactions between the Leu33 on the β2 strand and Tyr77 and Ile78 on the β6 loop of the ACD dimer should also be critical for the reduced stability of the L33S mutant. Similarly, the Leu33-Tyr77 hydrophobic interaction in *Tpv* HSP 14.3 is equivalent to Ile47-Tyr96 inter-subunit contact in the ACD of the MjHSP16.5 (from *Methanococcus jannaschii*) and analysis of its crystal structure suggested that this interaction can be involved in the stabilization of the MjHSP16.5 structure [25]. Thus, our result also complements the previous reports that proposed the hydrophobic interactions as the critical factors contributing to the thermal stability of thermophilic proteins [31].

The Y34F mutation did not alter hydrophobic interactions, and the change in the bond distances was not significant in the Y34F mutant relative to the WT sHSP, as well. Therefore, Y34 replacement by more hydrophobic F did not produce a dramatic effect on the solubility as well as the stability of the sHSP protein. Also, it is likely that Y34 to F substitution produced newly exposed hydrophobic surfaces on ACD, which could act as substrate binding sites. At the high chaperone concentrations (*i.e.*, 1:500 w/w substrate/sHSP ratio), both L33S and Y34F mutants performed 9 to 10% higher protection of the phCS activity as compared to positive control. However, the L33S sHSP was less efficient than the Y34F sHSP for protection of ADH at 1:90 w/w substrate/chaperone ratio and protection of the phCS at lower concentrations (*i.e.*, substrate/chaperone ratio of 1:147) from heat inactivation. The greater ability of Y34F compared with the L33S to

protect these two substrates can be hypothesized to arise from its increased hydrophobicity that may contribute to forming a hydrophobic surface. This result is compatible with previously published data suggesting that at higher temperatures, elevated chaperone activity of the sHSPs is mainly due to exposure of their buried hydrophobic patches which can readily capture aggregation-prone substrates [28, 32–34]. In parallel to our findings in *Drosophila melanogaster* Hsp27 and human CRYAB, mutations that involve substitutions by hydrophobic residues were found to be associated with altered surface properties and increased the chaperone activity [35, 36]. In mouse CRYAB, hydrophobicity at position 68 (M68) (which is equivalent to the L33 of *Tpv* HSP 14.3) was found to be important for chaperone function. Increasing hydrophobicity by replacing methionine with highly hydrophobic amino acids (Ile or Val) improved the chaperone activity, while decreasing hydrophobicity with polar residue substitution (Thr) reduced its activity [37].

In conclusion, this study sheds light on the dual importance of hydrophobic interactions at the dimer interface of *Tpv* HSP 14.3 for maintaining the structural/thermodynamic stability and effectiveness of the chaperone function. Our findings can contribute not only to understanding the molecular mechanisms behind sHSPs action but also to the affords for developing therapeutic strategies that target the diseases that result from protein misfolding and aggregation (e.g., cataract, Alzheimer's Disease, Parkinson's Disease)[1, 38–40].

5 ACKNOWLEDGEMENTS

The authors acknowledge METU-BAP for partially supporting this project with grants (TEZ-D-108-2020-10187).

6 AUTHOR CONTRIBUTIONS

Hypothesis: S.K., ; Design: S.K., S.Z.; Literature review: S.K., S.Z.; Data Collection: S.K., S.Z., A.R. ; Analysis and/or interpretation: S.K., S.Z.; Manuscript writing: S.K., S.Z.

7 CONFLICT OF INTEREST

The Authors declare that there is no conflict of interest.

8 REFERENCES

[1] Hu C et al. Heat shock proteins: Biological functions, pathological roles, and therapeutic opportunities. MedComm, 2022;3(3):1–39. DOI:10.1002/mco2.161

[2] Macario a J et al. Stress genes and proteins in the archaea. Microbiology and molecular biology reviews : MMBR, 1999;63(4):923–967. DOI: 10.1128/MMBR.63.4.923-967.1999

[3] Haslbeck M, Vierling E. A First Line of Stress Defense: Small Heat Shock Proteins and Their Function in Protein Homeostasis. Journal of Molecular Biology, 2015;427(7):1537–1548. DOI:10.1016/j.jmb.2015.02.002

[4] Tedesco B et al. Insights on Human Small Heat Shock Proteins and Their Alterations in Diseases. Frontiers in Molecular Biosciences, 2022;9:1–27. DOI:10.3389/fmolb.2022.842149

[5] Roy M, Bhakta K, Ghosh A. Minimal Yet Powerful: The Role of Archaeal Small Heat Shock Proteins in Maintaining Protein Homeostasis. Frontiers in Molecular Biosciences, 2022;9:1–9. DOI:10.3389/fmolb.2022.832160

[6] Haslbeck M, Weinkauf S, Buchner J. Small heat shock proteins: Simplicity meets complexity. Journal of Biological Chemistry, 2019;294:2121–2132. DOI:10.1074/jbc.REV118.002809

[7] Reinle K, Mogk A, Bukau B. The Diverse Functions of Small Heat Shock Proteins in the Proteostasis Network. Journal of Molecular Biology, 2021;434(1):167–157. DOI:10.1016/j.jmb.2021.167157

[8] Mogk A, Ruger-herreros C, Bukau B. Cellular Functions and Mechanisms of Action of Small Heat Shock Proteins. Annual Review of Microbiology, 2019;73:89–110. DOI:10.1146/annurev-micro-020518-115515

[9] Hayashi J, Carver JA. The multifaceted nature of αB-crystallin. Cell Stress and Chaperones,2020;25(4):639–654. DOI:10.1007/s12192-020-01098-w

[10] Mogk A, Bukau B. Role of sHsps in organizing cytosolic protein aggregation and disaggregation. Cell Stress and Chaperones,2017;22(4):493-502. DOI:10.1007/s12192-017-0762-4

[11] Hilario E et al. Crystal structures of xanthomonas small heat shock protein provide a structural basis for an active molecular chaperone oligomer. Journal of Molecular Biology, 2011;408(1):74–86. DOI:10.1007/s12192-017-0762-410.1016/j.jmb.2011.02.004

[12] Obuchowski I, Karaś P, Liberek K. The Small Ones Matter—sHsps in the Bacterial Chaperone Network. Frontiers in Molecular Biosciences, 2021;8:1–7. DOI:10.3389/fmolb.2021.666893

[13] Hilton GR et al. C-terminal interactions mediate the quaternary dynamics of αB-crystallin. Philosophical Transactions of the Royal Society B: Biological Sciences, 2013;368(1617):1–13. DOI:10.1098/rstb.2011.0405

[14] Clark a. R et al. Crystal structure of R120G disease mutant of human αB-crystallin domain dimer shows closure of a groove. Journal of Molecular Biology, 2011;408(1):118–134. DOI:10.1016/j.jmb.2011.02.020

[15] Kim M V et al. Structure and properties of K141E mutant of small heat shock protein HSP22 (HspB8, H11) that is expressed in human neuromuscular disorders. Archives of Biochemistry and Biophysics, 2006;454(1):32–41. DOI:10.1016/j.abb.2006.07.014

[16] Litt M et al. Autosomal dominant congenital cataract associated with a missense mutation in the human alpha crystallin gene CRYAA. Human Molecular Genetics, 1998;7(3):471–474. DOI:10.1093/hmg/7.3.471

[17] Vicart P et al. A missense mutation in the alphaB-crystallin chaperone gene causes a desmin-

related myopathy. Nature Genetics, 1998;20(1):92–95. DOI:10.1038/1765

[18] Kasakov AS et al. Effect of mutations in the β5-β7 loop on the structure and properties of human small heat shock protein HSP22 (HspB8, H11). FEBS Journal,2007;274:5628–5642. DOI:10.1111/j.1742-4658.2007.06086.x

[19] Quinlan RA et al.Changes in the quaternary structure and function of MjHSP16.5 attributable to deletion of the IXI motif and introduction of the substitution, R107G, in the α-crystallin domain. Philosophical Transactions of the Royal Society of London. Series B, Biological Sciences, 2013;368(1617):20120327. DOI:10.1098/rstb.2012.0327

[20] Kocabıyık S, Aygar S. Improvement of protein stability and enzyme recovery under stress conditions by using a small HSP (tpv-HSP 14.3) from Thermoplasma volcanium. Process Biochemistry, 2012;47(11):1676–1683. DOI:10.1016/j.procbio.2011.11.014

[21] Kagi JH, Vallee BL. The role of zinc in alcohol dehydrogenase. V. The effect of metal-binding agents on thestructure of the yeast alcohol dehydrogenase molecule. The Journal of Biological Chemistry, 1960;235:3188–3192. PMID: 13750715.

[22] Waterhouse AM et al. Jalview Version 2-A multiple sequence alignment editor and analysis workbench. Bioinformatics, 2009;25(9):1189–1191. DOI: 10.1093/bioinformatics/btp033

[23] Cheng J, Randall A, Baldi P. Prediction of protein stability changes for single-site mutations using support vector machines. Proteins: Structure, Function and Genetics, 2006;62(4):1125–1132. DOI: 10.1002/prot.20810

[24] Bigman LS, Levy Y. Entropic Contributions to Protein Stability. Israel Journal of Chemistry, 2020;60(7):705–712. DOI: 10.1002/ijch.202000032

[25] Kim KK, Kim R, Kim SH. Crystal structure of a small heat-shock protein. Nature, 1998;394(6693):595–599. DOI:10.1038/29106

[26] Liu L et al. Active-State Structures of a Small Heat-Shock Protein Revealed a Molecular Switch for Chaperone Function. Structure. 2015;23(11):2066–2075. http://dx.doi.org/10.1016/j.str.2015.08.015. DOI:10.1016/j.str.2015.08.015

[27] Hanazono Y et al. Structural Studies on the Oligomeric Transition of a Small Heat Shock Protein, StHsp14.0. Journal of Molecular Biology, 2012;422(1):100–108. DOI:10.1016/j.jmb.2012.05.017

[28] van Montfort RL et al. Crystal structure and assembly of a eukaryotic small heat shock protein. Nature Structural Biology, 2001;8(12):1025–1030. DOI:10.1038/nsb722

[29] Chen J, Shen B. Computational Analysis of Amino Acid Mutation: A Proteome Wide Perspective. Current Proteomics, 2009;6(4):228–234. DOI: 10.2174/157016409789973734

[30] Doss CGP, NagaSundaram N. Investigating the structural impacts of I64T and P311S mutations in APE1-DNA complex: A molecular dynamics approach. PLoS ONE,

2012;7(2):1–11. DOI:10.1371/journal.pone.0031677

[31] Goldstein RA. Amino-acid interactions in psychrophiles, mesophiles, thermophiles, and hyperthermophiles: Insights from the quasi-chemical approximation. Protein Science, 2007;16(9):1887–1895. DOI:10.1110/ps.072947007

[32] Das KP, Surewicz WK. Temperature-induced exposure of hydrophobic surfaces and its effect on the chaperone activity of α-crystallin. FEBS Letters, 1995;369:321–325. DOI: 10.1016/0014-5793(95)00775-5

[33] Kim R et al. On the mechanism of chaperone activity of the small heat-shock protein of Methanococcus jannaschii. Proceedings of the National Academy of Sciences of the United States of America, 2003;100(8):8151–8155. DOI: 10.1073/pnas.1032940100

[34] Bova MP, Huang Q, Ding L, Horwitz J. Subunit exchange, conformational stability, and chaperone-like function of the small heat shock protein 16.5 from Methanococcus jannaschii. Journal of Biological Chemistry, 2002;277(41):38468–38475. DOI: 10.1074/jbc.M205594200

[35] Moutaoufik MT et al. Oligomerization and chaperone-like activity of Drosophila melanogaster small heat shock protein DmHsp27 and three arginine mutants in the alpha-crystallin domain. Cell Stress and Chaperones, 2017;22:455–466. DOI:10.1007/s12192-016-0748-7

[36] Santhoshkumar P, Sharma KK. Conserved F84 and P86 residues in αB-crystallin are essential to effectively prevent the aggregation of substrate proteins. Protein Science, 2006;15:2488–2498. DOI: 10.1110/ps.062338206

[37] Shroff NP, Bera S, Cherian-Shaw M, Abraham EC. Substituted hydrophobic and hydrophilic residues at methionine-68 influence the chaperone-like function of αB-crystallin. Molecular and Cellular Biochemistry, 2001;220:127–133. DOI: 10.1023/A:1010834107809

[38] Zabci S. Therapeutic importance of small heat shock proteins and their interactions with other proteins In: Arıcı Y, Hancı H (ed).Multidisciplinary Approach to Basic and Clinical Science. Ankara:IKSAD International Publishing House; 2023:61-77.[ISBN: 978-625-367-203-4] https://iksadyayinevi.com/home/multidisciplinary-approach-to-basic-and-clinical-science/

[39] Mymrikov E V., Seit-Nebi AS, Gusev NB. Large potentials of small heat shock Proteins. Physiological Reviews, 2011;91(4):1123–1159. DOI:10.1152/physrev.00023.2010

[40] Muranova LK et al. Small Heat Shock Proteins and Human Neurodegenerative Diseases. Biochemistry, 2019;84(11):1256–1267. DOI: 10.1134/S000629791911004X

e-ISSN: 2980-0463
Anat. J. Pharm. Sci 2023:2(1)
AJPS
Research Article

Design And Development of A Prototype Of Programmable Tracheostomy Cannula That Can Perform Over-Cuff Suction For Use In Intensive Care Patients With Dysphagia

Kadir BATCIOGLU[1], Mehmet TECELLIOGLU[2*],

[1*] Department of Biochemistry, Faculty of Pharmacy, Inonu University, Malatya, Türkiye

[2] Department of Neurology, Faculty of Medicine, Inonu University, Malatya, Türkiye

ABSTRACT: One of the most significant risks in patients with respiratory device-related dysphagia is aspiration pneumonia. Due to the absence of a swallowing reflex in these patients, secretions from the mouth and nose can flow into the trachea, accumulating on the cuff. This creates a conducive environment for bacterial growth, leading to the development of pneumonia in the patient. Currently, nurses manually perform suctioning for these patients. However, manual aspiration falls short in providing the desired level of disinfection and cannot be performed as frequently as needed. In this study, a prototype tracheostomy cannula capable of spontaneous cuff washing and aspiration was developed to address these challenges.

Key Words: Tracheostomy, tracheostomy canula, dysphagia, aspiration pneumonia.

1 INTRODUCTION

Tracheostomy becomes unavoidable for patients in intensive care who are unconscious or suffer from dysphagia. In these cases, secretions with a mucoid consistency flow from the mouth and nose into the trachea, posing the risk of bronchial blockage [1]. To counteract this, cuffed cannulas have been developed. The cuff, an air-filled balloon surrounding the cannula, serves to prevent the downward passage of secretions. However, prolonged use of these cannulas may lead to necrosis on the tracheal wall over time due to cuff pressure [2]. To prevent such complications, the cuff should be deflated every 2 hours, allowing a 10-15 minute rest for the tracheal wall. Unfortunately, every time the cuff is deflated, secretions accumulated on the cuff in dysphagic patients flow into the bronchi, causing obstruction and elevating the risk of aspiration pneumonia [3].

*Corresponding Author: Kadir BATCIOGLU
E-mail: kadir.batcioglu@inonu.edu.tr
Submitted: 08.11.2023 Accepted: 30.10.2023

To mitigate this risk, it is crucial to regularly remove the secretions on the cuff and sterilize the area. Currently, this process is manually performed by nurses or auxiliary healthcare personnel in hospitals. Regrettably, in many cases, complete removal of secretions and full sterilization cannot be achieved. Consequently, a significant number of intensive care patients may succumb to aspiration pneumonia [4].

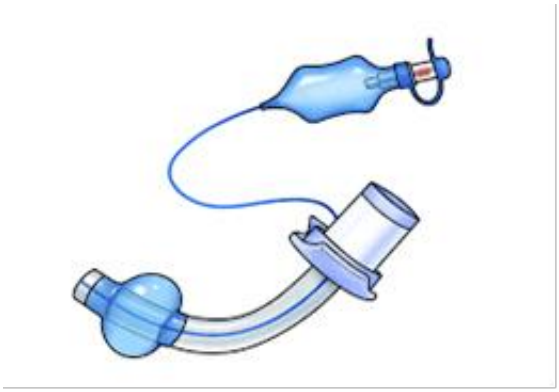

Figure 1. The classic cuffed cannula.

In the developed model, programming is facilitated through a digital control unit. As elaborated in the materials and methods section, this system periodically monitors the cuff pressure, administers antibiotic liquid above the cuff, allows time for aspiration, and subsequently deflates the cuff while giving the tracheal wall a necessary rest. This automated process not only yields labor savings but also minimizes potential errors inherent in manual applications. Most importantly, we anticipate a significant reduction in patient losses attributed to aspiration pneumonia.

2 MATERIAL AND METHOD

The placement of the cannula in the trachea and the connection between the cannula and the system are as shown in the Figure 2.

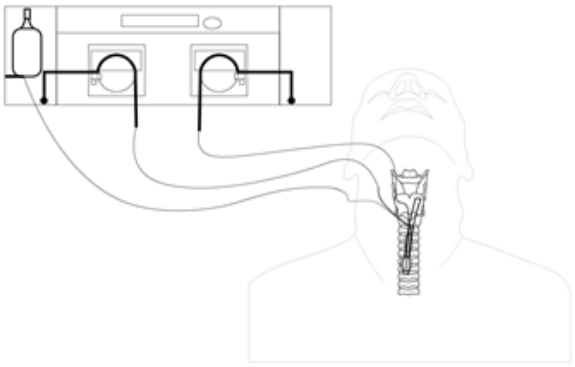

Figure 2. The system and cannula connections.

All components of the system and the functions of these components are shown in detail in figure 3.

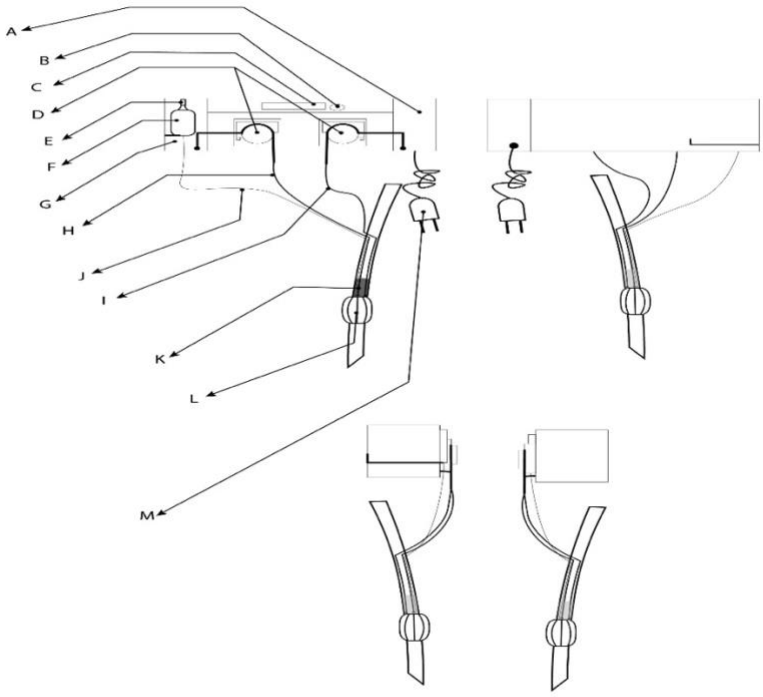

Figure 3. All system components. System Components; A: Reservoir for liquid bottles, B: Pressure, volume and time adjustment button, C: Digital Display, D: Pumps, E: Cuff inflation valve, F: Cuff pressure indicator bubble, G: Cuff pressure sensor, H and I: Liquid flow hoses, J: Air flow höse, K: Antibacterial polymer part, L: Air way, M: Electrical connection cable.

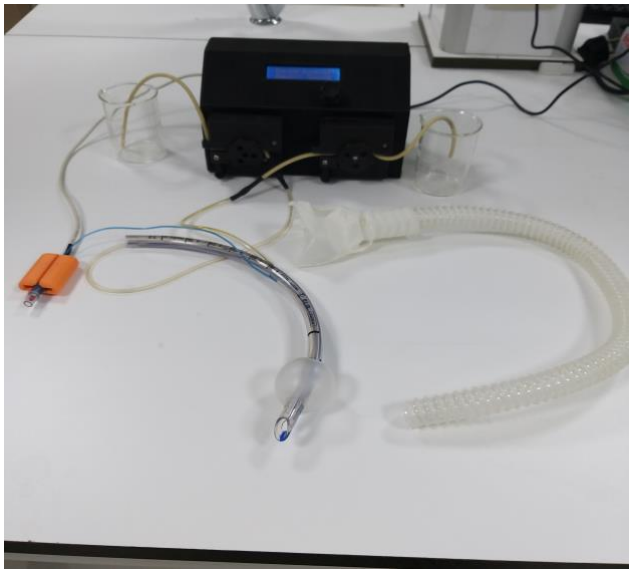

Figure 4. Prototype of the developed system

The fundamental operational principle of the device can be succinctly outlined as follows: following the insertion of the cannula integrated into the device into the trachea by a physician, the cuff is inflated, and air is supplied to the lungs either through connection to a respirator or via the patient's spontaneous breathing, if applicable. Upon reaching this point, the device is electrically connected and activated using the on/off button. Upon activation, the main menu appears on the screen, allowing the system to be programmed using the adjustment button. During this programming phase, parameters such as the quantity of antibacterial liquid the device will draw and dispense onto the cuff, the duration the liquid will remain in the environment above the cuff, the volume to be withdrawn, the number of repetitions within a specific time frame, the frequency of the process throughout the day, and the periodic repetition interval are set within the system. Additionally, the limit value for the cuff pressure is entered. Subsequently, one of the liquid flow hoses is connected to the antibacterial liquid container, while the other is linked to the container for collecting the liquid drawn after washing. The system is then initiated. Following the programmed time intervals, the system first checks the cuff pressure. If it falls below the entered limit value, it issues a warning to inflate the cuff. Conversely, if the pressure surpasses the limit value, the pump engages, releasing the antibacterial liquid onto the cuff in the predetermined volume. This liquid is recirculated within that region for the programmed duration. After this time period elapses, the second pump activates, drawing and transferring the liquid to the collection bottle at the end of the hose. This entire process is repeated as per the programmed specifications, ensuring optimal functionality.

3 RESULT AND DISCUSSION

The tracheostomy procedure plays a crucial role in the management of unconscious or dysphagic patients in intensive care. However, it brings about challenges, especially concerning the use of cuffed cannulas. While these cannulas effectively prevent the downward flow of secretions into the bronchi, they also present risks, such as tracheal wall necrosis with prolonged use. To address these risks, regular cuff deflation and resting of the tracheal wall are recommended. Unfortunately, the manual deflation and secretion removal process by healthcare personnel often falls short, increasing the risk of aspiration pneumonia and, regrettably, patient fatalities [5,6].

In response to these challenges, our developed model introduces an innovative solution that automates and optimizes the management of cuffed cannulas. Controlled by a digital unit, the system's primary functions include monitoring cuff pressure, administering antibiotic liquid above the cuff, aspirating the liquid, and subsequently deflating the cuff to allow the tracheal wall to rest. By automating these critical tasks, our model offers several advantages, such as reducing the workload of healthcare professionals and minimizing the potential for human error. In the literature, there is a study detailing a different model with similar characteristics that has been developed to address existing problems [7].

One of the primary objectives of our model is to substantially decrease patient losses attributed to aspiration pneumonia. By maintaining precise control over cuff pressure and consistently aspirating and sterilizing the area above the cuff, we aim to enhance patient safety. The automated nature of the system ensures that these tasks are performed at regular intervals, mitigating the potential for lapses in care and improving the overall quality of patient management. Furthermore, additional research and clinical studies will be necessary to validate the long-term effectiveness and safety of this system in practical healthcare settings.

In conclusion, our developed model offers a promising solution to improve the management of cuffed cannulas in tracheostomized patients, potentially reducing the risk of aspiration pneumonia and enhancing patient outcomes. While this system represents a significant advancement, ongoing research and testing are essential to validate its efficacy and safety.

4 ACKNOWLEDGMENTS

This study was financially supported by IUBAP within the scope of the project coded TKP-2020-1766

5 AUTHOR CONTRIBUTIONS

Authors have 50% contribution in all stages of the study and preparation of the article.

6 REFERENCES

[1] Wallace S, McGrath BA. Laryngeal complications after tracheal intubation and tracheostomy. BJA Educ. 2021; 21(7): 250–257.

[2] Del Negro MS, Barreto G, Antonelli RQ, Baldasso TA, Meireles LR, Moreira MM, Tincani AJ. Effectiveness of the endotracheal tube cuff on the trachea: physical and mechanical aspects. Rev Bras Cir Cardiovasc. 2014; 29(4): 552–558.

[3] Bone DK, Davis LJ, Zuidema DG, Cameron JL. Aspiration Pneumonia: Prevention of Aspiration in Patients with Tracheostomies. The Annals of Thoracic Surgery. 1974; 18(1):30-37.

[4] Dongho S, Gerald L, Lin RJ. In-hospital mortality for aspiration pneumonia in a tertiary teaching hospital: A retrospective cohort review from 2008 to 2018. Journal of Otolaryngology - Head & Neck Surgery. 2023; 52(23):4425-30.

[5] Smith, J. et al. The Importance of Tracheostomy in Critical Care: A Comprehensive Review. Journal of Intensive Care Medicine. 2019; 45(2): 87-95.

[6] Johnson, A. et al. Complications and Challenges Associated with Cuffed Tracheostomy Cannulas: A Retrospective Study. Critical Care Nursing Journal. 2020; 55(4): 212-225.

[7] Anderson, L. et al. An Automated System for Managing Cuffed Tracheostomy Cannulas in Intensive Care: A Novel Approach. Medical Engineering and Technology Journal. 2022; 70(6): 324-35.

[8] Garcia, E. et al. The Impact of an Automated System on Reducing Aspiration Pneumonia Incidence in Tracheostomy Patients: Preliminary Findings. Healthcare Innovation Research Journal. 2023; 75(2)88-101.

AJPS
e-ISSN: 2980-0463
Anat. J. Pharm. Sci 2023:2(1)
Review Article

Biochemistry of the Human Lens

Özlem Çankaya*

*Inonu University, Faculty of Pharmacy, Department of Biochemistry, 44280, Malatya, Türkiye

ABSTRACT: The main function of the crystalline lens is to transmit and focus light onto the retina by accommodation, just like the lens in a camera. At the beginning of embryonic life, the lens is opaque, but it becomes transparent over time as a result of nutrition. The main reasons for its transparency are the hexagonal structure of the fibrils, which are the main structural elements of the lens, and very little intercellular space. Lens transparency is maintained at both the cellular and molecular levels. The transparency of the lens is largely due to the very regular arrangement of the macromolecular components of the lens cells and the very small refractive index differences in the light-scattering components. The loss of the transparency of the lens is known as a cataract.

Maintaining cellular homeostasis between protein and carbohydrate metabolism, cell division, cell differentiation, oxidative damage and protective mechanisms supports the maintenance of lens transparency. Regulation of water and electrolyte balance plays a critical role in maintaining normal lens water content and transparency. As a result of the regression of the tunica vasculosa lentis, which nourishes the lens during intrauterine life, the lens obtains its metabolic requirements from the aqueous humour and vitreous humour.

Keywords: *Human Lens, lens biochemistry, human eye.*

1 INTRODUCTION

Up to 60% of the total mass of the lens may consist of proteins, much higher than in almost any other tissue. The lens is covered by a collagen capsule. The capsule acts as a barrier to diffusion and contributes to the remodelling of the lens during accommodation. Its major components are type IV collagen, laminin, entactin, perlecan, type XVIII collagen, heparin sulphate, proteoglycan and fibronectin. The capsular filaments, which are uniform in size and parallel in orientation, are thinnest at the posterior pole and reach their maximum thickness at the equator, where the lens zonules are located. The lens capsule first appears in humans at 5-6 weeks of gestation and is

*Corresponding Author: Ozlem CANKAYA
E-mail: ozlem.isikgil@inonu.edu.tr
Submitted: 25.11.2023 Accepted: 04.12.2023

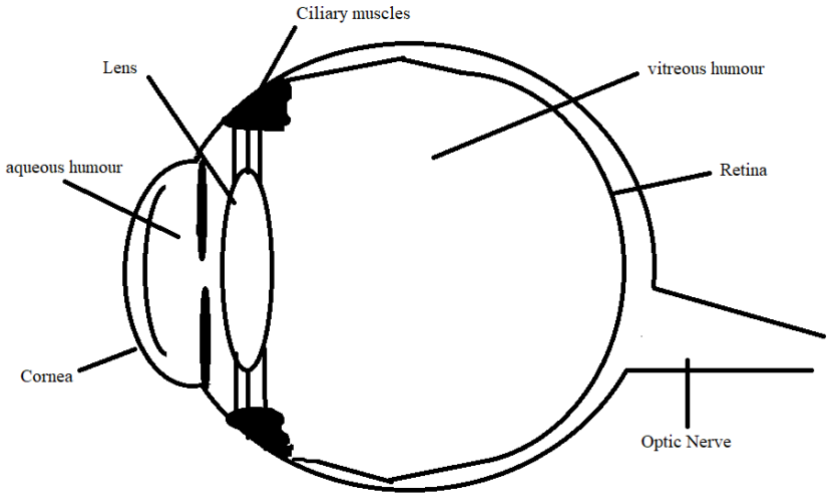

Figure 1. Human eye schematic

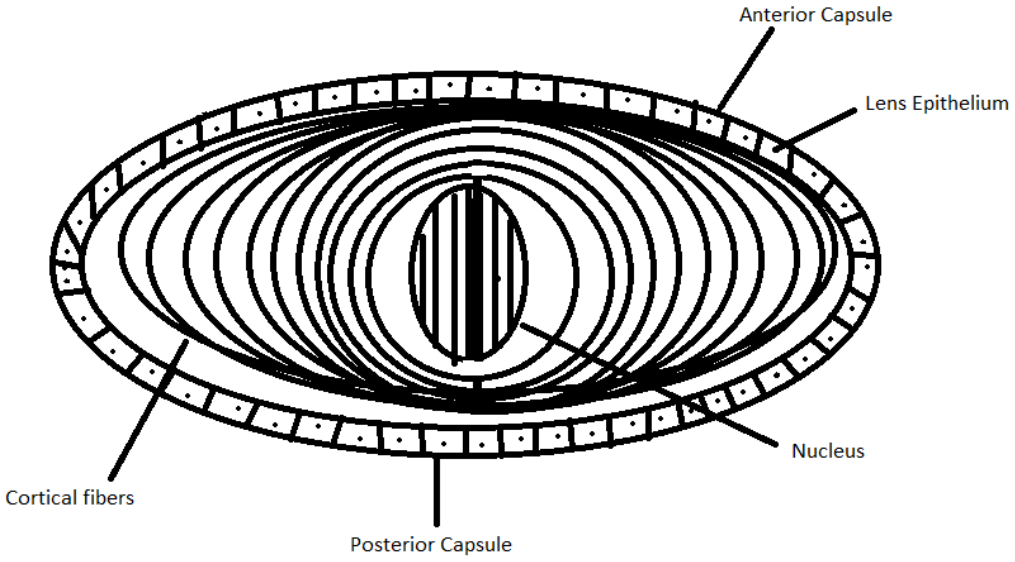

Figure 2. Lens Capsule, Epithelial Cells and Lens Fibrils

continuously produced throughout life, anteriorly by cuboidal epithelium and more slowly posteriorly by fibre cells (Figure 1,2) [1-3].

Except for a few tissues and organs in our body, nutrition is generally provided by the blood vessels. Fenestrated capillaries extend into the tissues and carry the oxygen

that the tissues need with the erythrocytes and the nutrients with the serum part of the blood. After receiving the metabolites it needs, the tissue returns the residues through the fenestrated capillaries and lymphatic vessels. The lens is one of the few structures in the body that is not actively circulated and maintains its own vitality. It relies on the aqueous humour for nutrition and waste removal. The metabolism of the lens therefore has a specialised cycle. The basic building block of all organs and tissues in the body is protein. The lens is one of the tissues with the highest protein content by volume in the body. The high protein content provides the high refractive index required by the lens. At the same time, lens proteins play an important role in maintaining the transparency of the lens. They are also responsible for the exchange of substances between the lens cells. Proteins within the lens cells are involved in maintaining cell shape [4,5].

In this review, we aim to focus on how the human lens reflects light and maintains its transparency through biochemical reactions.

2 METOBOLISM OF THE LENS

2.1 Carbohydrate Metabolism

Much of the energy production in the lens is provided by glucose metabolism. Glucose is imported into the lens from the aqueous humour by simple diffusion and facilitated diffusion. Most of the glucose that enters the lens is converted to glucose-6-phosphate by the enzyme hexokinase. The amount of glycolysis is limited by the amount of hexokinase. With age, the hexokinase enzyme decreases and energy production decreases. As a result, control of electrolyte metabolism becomes difficult. Glucose-6-phosphate is mainly used in two different metabolic pathways.

2.1.1 Anaerobic Glycolysis Pathway: 78% of glucose enters this pathway. The end product of this pathway is lactate. In this pathway, 2 ATP is formed from each glucose molecule. 70% of the energy requirements of the lens are

met by anaerobic glycolysis. Due to the low oxygen pressure in the lens, only 3% of the glucose enters the citric acid cycle. Nevertheless, the citric acid cycle provides 25% of the ATP requirement of the lens.

2.1.2 Hexose Monophosphate Pathway: Also known as the pentose phosphate pathway. Five percent of lens glucose enters this pathway. This pathway is usually stimulated by elevated glucose levels. The importance of this pathway is the formation of nicotinamide adenine dinucleotide phosphate (NADPH). In the lens, NADPH is required for the activities of glutathione reductase and aldose reductase. Aldose reductase is a key enzyme in the sorbitol pathway, another pathway of glucose metabolism.

Another pathway used in glucose metabolism is the sorbitol pathway, and 5% of the glucose in the lens enters this pathway. In this pathway, glucose is converted to sorbitol by the enzyme aldose reductase and then to fructose, which can diffuse into the aqueous humour by polyol dehydrogenase. The affinity of aldose reductase for glucose is much lower than that of hexokinase. As the glucose level in the lens increases, the sorbitol pathway is activated more than the glycolysis pathway and the formation of sorbitol and fructose, the end products of this pathway, increases in the lens. At the same time, the hexose monophosphate pathway is also stimulated, further contributing to the increase in aldose reductase activity required for sorbitol formation. As the permeability of the lens to sorbitol is low, sorbitol accumulates in the lens. With the increase in osmotic pressure, water enters the lens, resulting in swelling of the fibrils, changes in lens structure and opacification. This mechanism is known to play an important role in the development of diabetic cataract [6-9].

2.2 Energy Production in the Lens

Due to the lack of blood circulation, the concentration of oxygen in and around the lens is much lower than in other parts of the body. The lens therefore relies on glycolytic metabolism to produce most of its ATP. The

glucose required for glycolytic metabolism is derived from the aqueous humour. Aqueous glucose levels are maintained by facilitated diffusion across the ciliary epithelium. However, lens epithelial cells and superficial fibre cells also contain mitochondria. Therefore, cells near the lens surface use both glycolytic and oxidative pathways to obtain energy from glucose [10].

2.3. Protein Metabolism

Proteins make up about 33% of the weight of the lens. The lens has the highest protein content in the human body. There are two main types of protein: soluble crystalline and insoluble albuminoid. Water-soluble proteins are found inside the cell, while water-insoluble proteins are found in the membranes of the lens fibres. There are 3 groups of soluble crystallins. These are the alpha, beta and gamma fractions. Beta-crystallins are the most abundant (55%). Alpha crystallins account for 32% of water-soluble proteins. Gamma crystallins make up 15%. Alpha-crystallin has the largest molecular structure, is formed before birth, is present throughout life and is known as the embryonic lens protein and is closely related to the non-water soluble albuminoids. In young people, the amount of alpha-crystallin is highest in the cortex and the amount of albuminoids is highest in the nucleus. With age, alpha-crystallin decreases and albuminoids increase. With age, the rate of water-insoluble protein increases, leading to the formation of aggregates. This results in lens opacities that cause more light to be scattered. Over time, the total amount of protein in the lens decreases. This decrease is more pronounced in eyes with cataracts. With age, the polypeptides degrade, dissolve and lose their sulfhydryl groups. As a result, the lens becomes less transparent. While the ratio of water-soluble proteins in a clear adult lens is 81%, this ratio is only 51.4% in a cataractous lens. This suggests a loss of crystallin from the lens capsule [11-14].

2.4 Lens Lipids

Most lens lipids are associated with the cell membrane. Lens lipids are mostly found in the

protein-lipid complex. The lipids found in the lens are cholesterol, phospholipids and glycosphingolipids. The major phospholipid of the lens cell membrane is sphingomyelin. The combination of high levels of cholesterol and sphingomyelin makes the lens cell membrane more stable [15].

2.5 Water and Electrolyte Balance of the Lens

Electrolyte and water balance, which is essential for maintaining lens transparency, is the most important topic in lens physiology. Disturbances in cellular hydration lead to lens opacity. The lens cortex is more hydrated than the nucleus. The lens contains high levels of potassium ions and amino acids, unlike the aqueous and vitreous humours. In contrast, the lens contains less sodium ions, chlorine ions and water than the surrounding structures. The maintenance of this cation balance depends on the permeability properties of the lens cell membrane and the activity of the sodium pump. The function of the sodium pump is to release sodium ions and take up potassium ions. This mechanism is triggered by the breakdown of ATP, which is controlled by the enzyme Na-K-ATPase. Na-K-ATPase activity is most intense in lens epithelial cells and superficial cortical fibre cells. Inhibition of the Na-K-ATPase enzyme results in an imbalance of cations and an increase in the water content of the lens. The combination of active transport and cell membrane permeability is considered to be the pumpless system of the lens. According to the pump-less theory, various molecules such as potassium and amino acids are taken up from the aqueous humour by the epithelial cells in the anterior part of the lens. They are then transported to the posterior part of the lens by passive diffusion due to the difference in concentration, without an active transport mechanism. Most of the passive diffusion in the lens content is provided by the low resistance gap junctions between the cells. However, the opposite transport is observed for sodium ions. Due to the unilateral electrolyte distribution along the cell membrane, there is an electrical potential

difference between the inside and outside of the lens. The inside of the lens is electronegative at approximately -70 millivolts. There is a potential difference of -23 millivolts between the anterior and posterior sides of the lens. Calcium hemostasis is also very important for the lens. The difference in calcium concentration between intracellular and extracellular calcium is mainly provided by Ca-ATPase. Disruption of calcium hemostasis can cause damage to lens metabolism. There may be some adverse changes such as impaired glucose metabolism, formation of high molecular weight protein aggregates, destructive protease activation due to high calcium levels. Cell membrane permeability and active transport are important for lens nutrition. With the concentration difference created by sodium pumps, amino acids in the lens epithelium are transported into the lens by active transport. Glucose is delivered directly to the lens by facilitated diffusion, where active transport is not involved [16-19].

2.6 Oxidative Damage and Protective Mechanisms in the Lens

Free radicals are formed as a result of normal cellular metabolic activity in the lens. Free radicals can also be produced by external factors such as radiant (electromagnetic) energy from the sun. These highly reactive free radicals can damage the lens fibres and are thought to be one of the causes of lens opacity. During lipid peroxidation, the oxidant converts saturated fatty acids into radical fatty acids by removing the hydrogen atom. The fatty acid radical is converted to a lipid peroxy radical by binding to molecular oxygen. During this chain reaction, lipid peroxy (LOOH) is formed. LOOH is then converted to malondialdehyde (MDA), a potent cross-linking agent. Because of the low oxygen pressure in and around the lens, free radicals react directly with other molecules instead of molecular oxygen. DNA is easily damaged by free radicals. Some of the damage in the lens can be repaired and some cannot. Free radicals damage proteins in the cortex and lipids in the cell membrane. There

is no repair mechanism to correct this damage, which increases over time. In the lens fibres, where protein synthesis can no longer take place, free radicals cause polymerisation and cross-linking of lipids and proteins. This increases the amount of water-insoluble protein in the lens.

Oxidation-reduction mechanisms are particularly important in the lens. Oxidative damage leads to many molecular changes and contributes to the development of cataracts. Glutathione plays a very important role in protecting against this damage. Almost all glutathione in the lens is in reduced form (GSH). It has functions such as protecting thiol groups in proteins, preventing protein aggregation between disulfide bonds, and protecting sulfhydryl groups necessary for normal cation transport. Glutathione levels are significantly reduced in human and experimental cataracts. The lens becomes susceptible to oxidative damage. Glutathione is the major antioxidant in the lens. It exerts its antioxidant effect by detoxifying H2O2 and organic peroxides through reactions in which the enzyme glutathione peroxidase acts as a cofactor. The enzyme superoxide dismutase (SOD) is also present in the lens. Although it is found in high concentrations in normal lenses, its concentration decreases in cataractous lenses [20-24].

3 CONCLUSION

As a result, the human lens must maintain a healthy biochemical structure in order to maintain its transparency and its role in the visual system. Damage to the lens biochemistry, which can occur as a result of oxidation, leads to deterioration of the lens transparency and permanent damage to the visual system.

4 AUTHOR CONTRIBUTIONS

Hypotesis: Ö.Ç.; Design: Ö.Ç.; Literature review: Ö.Ç.; Data Col”lection: Ö.Ç.; Analysis and/or interpretation: Ö.Ç.; Manuscript writing: Ö.Ç.

5 CONFLICT OF INTEREST

Authors declare that there is no conflict of interest.

6 REFERENCES

[1] Wistow GJ, Piatigorsky J. Lens crystallins: the evolution and expression of proteins for a highly specialized tissue. *Annu Rev Biochem,* 1988;57:479–504.

[2] Danysh BP, Duncan MK. The lens capsule. *Exp Eye Res,* 2009;88(2):151–164.

[3] Koretz JF, Handelman GH. How the human eye focuses. *Sci Am,* 1988;256:92–99.

[4] Alikma MS, Erkul SO, Unsal E. Lens Proteins and Physiology. *Med J SDU*, 2018:25(3):342-348.

[5] Andley UP. Crystallins in the eye: Function and pathology. *Progress in retinal and eye research,* 2007;26(1):78-98.

[6] Hockwin O, Fink H, Glasmacher M. Carbohydrate metabolism of the lens depending on age. *Z Alternsforsch,* 1976;31(6):521-35.

[7] Bron AJ, Brown NA, Harding JJ, Ganea E. The lens and cataract in diabetes. *Int Ophthalmol Clin,* 1998 Spring;38(2):37-67.

[8] Preda M. The characteristics of crystalline lens metabolism. *Oftalmologia*, 1997;41(1):8-11.

[9] Green H, Bocher CA, Leopold IH. Anaerobic carbohydrate metabolism of the crystalline lens. I. Glucose and glucose-6-phosphate. *Am J Ophthalmol*, 1955 Feb;39(2 Pt 2):106-13.

[10] Augusteyn RC. On the growth and internal structure of the human lens. *Exp Eye Res*, 2010 Jun;90(6):643-54.

[11] Norton-Baker B, Mehrabi P, Kwok AO, Roskamp KW, Rocha MA, Sprague-Piercy MA, von Stetten D, Miller RJD, Martin RW. Deamidation of the human eye lens protein γS-crystallin accelerates oxidative aging. *Structure,* 2022 May 5;30(5):763-776.

[12] Michael R, Bron AJ. The ageing lens and cataract: a model of normal and pathological ageing. *Philos Trans R Soc Lond B Biol Sci*, 2011 Apr 27;366(1568):1278-92.

[13] Reddy VN, Giblin FJ. Metabolism and function of glutathione in the lens. *Ciba Found Symp*, 1984;106:65-87.

[14] Zhang K, Zhu X, Lu Y. The Proteome of Cataract Markers: Focus on Crystallins. *Adv Clin Chem*, 2018;86:179-210.

[15] Choudhary S, Srivastava S, Xiao T, Andley UP, Srivastava SK, Ansari NH. Metabolism of lipid derived aldehyde, 4-hydroxynonenal in human lens epithelial cells and rat lens. *Invest Ophthalmol Vis Sci,* 2003 Jun;44(6):2675-82.

[16] Harris JE, Gruber L. The electrolyte and water balance of the lens. *Exp Eye Res*, 1962 Jun;1:372-84.

[17] Wilson CC, Delamere NA, Paterson CA. Chlorpromazine effects upon rabbit lens water and electrolyte balance. *Exp Eye Res*, 1983 Apr;36(4):559-65.

[18] Sanders D, Peyman G, McClellan K. Dextran 40-containing incubation media: effect on lens electrolyte and water balance. *Arch Ophthalmol,* 1979 Jan;97(1):156-8.

[19] Fischbarg J. Water channels and their roles in some ocular tissues. *Mol Aspects Med,* 2012 Oct-Dec;33(5-6):638-41.

[20] Lim JC, Caballero Arredondo M, Braakhuis AJ, Donaldson PJ. Vitamin C and the Lens: New Insights into Delaying the Onset of Cataract. *Nutrients*, 2020 Oct 14;12(10):3142.

[21] Hsueh YJ, Chen YN, Tsao YT, Cheng CM, Wu WC, Chen HC. The Pathomechanism, Antioxidant Biomarkers, and Treatment of Oxidative Stress-Related Eye Diseases. *Int J Mol Sci,* 2022 Jan 23;23(3):1255.

[22] Muranov KO, Ostrovsky MA. Biochemistry of Eye Lens in the Norm and in Cataractogenesis. *Biochemistry (Mosc),* 2022 Feb;87(2):106-120.

[23] Johra FT, Bepari AK, Bristy AT, Reza HM. A Mechanistic Review of β-Carotene, Lutein, and Zeaxanthin in Eye Health and Disease. *Antioxidants (Basel)*, 2020 Oct 26;9(11):1046.

[24] Lou MF. Glutathione and Glutaredoxin in Redox Regulation and Cell Signaling of the Lens. *Antioxidants (Basel)*, 2022 Oct 1;11(10):1973.